

EUR 5078 e

COMMISSION OF THE EUROPEAN COMMUNITIES

**SELF-DIFFUSION OF URANIUM IN URANIUM
MONOCARBIDE-EVALUATION OF
CURVED ARRHENIUS DIAGRAMS**

by

HJ. MATZKE and H.A. TASMAN

1974



Joint Nuclear Research Centre
Karlsruhe Establishment - Germany
European Institute for Transuranium Elements

LEGAL NOTICE

This document was prepared under the sponsorship of the Commission of the European Communities.

Neither the Commission of the European Communities, its contractors nor any person acting on their behalf:

make any warranty or representation, express or implied, with respect to the accuracy, completeness, or usefulness of the information contained in this document, or that the use of any information, apparatus, method or process disclosed in this document may not infringe privately owned rights; or

assume any liability with respect to the use of, or for damages resulting from the use of any information, apparatus, method or process disclosed in this document.

This report is on sale at the addresses listed on cover page 4

at the price of B.Fr. 70.—

**Commission of the
European Communities
D.G. XIII - C.I.D.
29, rue Aldringen
Luxembourg
February 1974**

This document was reproduced on the basis of the best available copy.

EUR 5078 e

SELF-DIFFUSION OF URANIUM IN URANIUM MONOCARBIDE-EVALUATION OF CURVED ARRHENIUS DIAGRAMS

by Hj. MATZKE and H.A. TASMAN

Commission of the European Communities

Joint Nuclear Research Centre — Karlsruhe Establishment (Germany)
Luxembourg, February 1974 — 52 Pages — 26 Figures — B.Fr. 70.—

Curved Arrhenius plots have been observed before in diffusion work on a number of systems. The mathematical attributions of diffusion constants to a high and a low temperature process were always cumbersome and often arbitrary. A curved Arrhenius plot has now also been observed for uranium diffusion in stoichiometric uranium monocarbide, UC. For an optimal evaluation, either two separate or the sum of two exponentials were fitted to the experimental data. For the latter case, an iterative procedure showed that the standard deviation σ is rather insensitive to considerable variations in slopes and intercepts. Acceptable results are obtained, however, with a minimization of σ

EUR 5078 e

SELF-DIFFUSION OF URANIUM IN URANIUM MONOCARBIDE-EVALUATION OF CURVED ARRHENIUS DIAGRAMS

by Hj. MATZKE and H.A. TASMAN

Commission of the European Communities

Joint Nuclear Research Centre — Karlsruhe Establishment (Germany)
Luxembourg, February 1974 — 52 Pages — 26 Figures — B.Fr. 70.—

Curved Arrhenius plots have been observed before in diffusion work on a number of systems. The mathematical attributions of diffusion constants to a high and a low temperature process were always cumbersome and often arbitrary. A curved Arrhenius plot has now also been observed for uranium diffusion in stoichiometric uranium monocarbide, UC. For an optimal evaluation, either two separate or the sum of two exponentials were fitted to the experimental data. For the latter case, an iterative procedure showed that the standard deviation σ is rather insensitive to considerable variations in slopes and intercepts. Acceptable results are obtained, however, with a minimization of σ

EUR 5078 e

SELF-DIFFUSION OF URANIUM IN URANIUM MONOCARBIDE-EVALUATION OF CURVED ARRHENIUS DIAGRAMS

by Hj. MATZKE and H.A. TASMAN

Commission of the European Communities

Joint Nuclear Research Centre — Karlsruhe Establishment (Germany)
Luxembourg, February 1974 — 52 Pages — 26 Figures — B.Fr. 70.—

Curved Arrhenius plots have been observed before in diffusion work on a number of systems. The mathematical attributions of diffusion constants to a high and a low temperature process were always cumbersome and often arbitrary. A curved Arrhenius plot has now also been observed for uranium diffusion in stoichiometric uranium monocarbide, UC. For an optimal evaluation, either two separate or the sum of two exponentials were fitted to the experimental data. For the latter case, an iterative procedure showed that the standard deviation σ is rather insensitive to considerable variations in slopes and intercepts. Acceptable results are obtained, however, with a minimization of σ

while varying one or two of the parameters steps and adjusting the remaining parameters.

The resulting equation for the diffusion of U in UC is $D = 6.9 \exp(-141.000/RT) + 3.6 \times 10^{-5} \exp(-84.500/RT) \text{ cm}^2 \text{ sec}^{-1}$. These results are discussed on basis of the present knowledge of nontrivial curved Arrhenius diagrams (so far observed mainly for metals, alkali and silver halides). Different possible mechanisms are discussed. As plausible reason for the curvature, a single vacancy mechanism is suggested at low temperatures, whereas a divacancy mechanism is said to dominate at temperatures near the melting point (2085 - 2545°C). The present knowledge on carbides does, however, not suffice to definitely exclude other alternatives. As most probable alternative, the effect of impurities by providing impurity-vacancy interactions is suggested.

Finally, the evaluation procedure was applied to curved Arrhenius-plots on other systems that were reported in the literature.

while varying one or two of the parameters steps and adjusting the remaining parameters.

The resulting equation for the diffusion of U in UC is $D = 6.9 \exp(-141.000/RT) + 3.6 \times 10^{-5} \exp(-84.500/RT) \text{ cm}^2 \text{ sec}^{-1}$. These results are discussed on basis of the present knowledge of nontrivial curved Arrhenius diagrams (so far observed mainly for metals, alkali and silver halides). Different possible mechanisms are discussed. As plausible reason for the curvature, a single vacancy mechanism is suggested at low temperatures, whereas a divacancy mechanism is said to dominate at temperatures near the melting point (2085 - 2545°C). The present knowledge on carbides does, however, not suffice to definitely exclude other alternatives. As most probable alternative, the effect of impurities by providing impurity-vacancy interactions is suggested.

Finally, the evaluation procedure was applied to curved Arrhenius-plots on other systems that were reported in the literature.

while varying one or two of the parameters steps and adjusting the remaining parameters.

The resulting equation for the diffusion of U in UC is $D = 6.9 \exp(-141.000/RT) + 3.6 \times 10^{-5} \exp(-84.500/RT) \text{ cm}^2 \text{ sec}^{-1}$. These results are discussed on basis of the present knowledge of nontrivial curved Arrhenius diagrams (so far observed mainly for metals, alkali and silver halides). Different possible mechanisms are discussed. As plausible reason for the curvature, a single vacancy mechanism is suggested at low temperatures, whereas a divacancy mechanism is said to dominate at temperatures near the melting point (2085 - 2545°C). The present knowledge on carbides does, however, not suffice to definitely exclude other alternatives. As most probable alternative, the effect of impurities by providing impurity-vacancy interactions is suggested.

Finally, the evaluation procedure was applied to curved Arrhenius-plots on other systems that were reported in the literature.

EUR 5078 e

COMMISSION OF THE EUROPEAN COMMUNITIES

**SELF-DIFFUSION OF URANIUM IN URANIUM
MONOCARBIDE-EVALUATION OF
CURVED ARRHENIUS DIAGRAMS**

by

HJ. MATZKE and H.A. TASMAN

1974



Joint Nuclear Research Centre
Karlsruhe Establishment - Germany
European Institute for Transuranium Elements

ABSTRACT

Curved Arrhenius plots have been observed before in diffusion work on a number of systems. The mathematical attributions of diffusion constants to a high and a low temperature process were always cumbersome and often arbitrary. A curved Arrhenius plot has now also been observed for uranium diffusion in stoichiometric uranium monocarbide, UC. For an optimal evaluation, either two separate or the sum of two exponentials were fitted to the experimental data. For the latter case, an iterative procedure showed that the standard deviation σ is rather insensitive to considerable variations in slopes and intercepts. Acceptable results are obtained, however, with a minimization of σ while varying one or two of the parameters steps and adjusting the remaining parameters.

The resulting equation for the diffusion of U in UC is $D = 6.9 \exp(-141.000/RT) + 3.6 \times 10^{-5} \exp(-84.500/RT) \text{ cm}^2 \text{ sec}^{-1}$. These results are discussed on basis of the present knowledge of nontrivial curved Arrhenius diagrams (so far observed mainly for metals, alkali and silver halides). Different possible mechanisms are discussed. As plausible reason for the curvature, a single vacancy mechanism is suggested at low temperatures, whereas a divacancy mechanism is said to dominate at temperatures near the melting point (2085 - 2545°C). The present knowledge on carbides does, however, not suffice to definitely exclude other alternatives. As most probable alternative, the effect of impurities by providing impurity-vacancy interactions is suggested.

Finally, the evaluation procedure was applied to curved Arrhenius-plots on other systems that were reported in the literature.

KEYWORDS

SELF-DIFFUSION
URANIUM CARBIDES
ARRHENIUS EQUATION
REACTION KINETICS
VACANCIES
IMPURITIES

	page
1. Introduction	5
2. Experimental	6
3. Results	8
4. Evaluation of the Non-Linear Arrhenius Diagram	12
5. Discussion	
5.1. Summary of Literature Data on Curved Arrhenius	
5.1.1 Alkali Halides	22
Plots	
5.1.2 Silver Halides	23
5.1.2 Fcc Metals	24
5.1.4 "Anomalous" bcc Metals	25
5.2. Properties of Point Defects in UC	31
5.3. Possible Divacancy Contribution to Uranium Self-	32
Diffusion in UC	
6. Conclusions and Summary	33
References	38
Appendix I : Recalculation of Literature Data on	40
Curved Arrhenius Plots	

1. Introduction

In most diffusion studies, diffusion coefficients are given as function of temperature, T (in $^{\circ}\text{K}$), using the conventional Arrhenius relation

$$D = D_0 \exp(-\Delta H/RT) \quad (1)$$

with R = gas constant, where both the activation enthalpy of diffusion, ΔH , and the pre-exponential factor, D_0 , are assumed to be temperature independent. Hence, the data are fitted to a straight line in a plot of $\log D$ versus $1/T$.

Such a treatment, however, is not always justified. There are both trivial reasons for deviations from straight lines^{a)} which can be excluded by proper choice of the experimental conditions, and inherent causes for a curvature in the Arrhenius diagram. These latter include i) a temperature dependence of ΔH itself or ii) the contribution of more than one intrinsic mechanism to volume diffusion.

Most of the present knowledge of these phenomena is restricted to metals, (see review in ref. (1)). The available data and estimates indicate that the temperature dependences of both formation and migration energies of single vacancies in close-packed metals are quite small, and that rather noticeable contributions of divacancies to the overall volume diffusion may exist at high temperatures. Hence, the resulting experimental diffusion coefficient, D_{exp} , would be given by

$$D_{\text{exp}} = D_{0,1} \exp(-\Delta H_1/RT) + D_{0,2} \exp(-\Delta H_2/RT) \quad (2)$$

where the indices 2 and 1 stand for the diffusion constants of single and divacancies, respectively. Divacancy contributions to self diffusion have further been demonstrated or postulated in alkali halides.

a) footnote : The trivial reasons are deviations from volume diffusion due to contributions at low temperatures of fast diffusion paths as dislocation lines and/or grain boundaries etc., or the existence of phase changes within the investigated temperature range.

Very pronounced curvatures in the Arrhenius plots have also been observed for self-diffusion and impurity diffusion in some bcc metals (which are referred to as "anomalous" bcc metals). Despite a tremendous amount of work performed on these metals in the past few years, no unique interpretation for their diffusion behavior can be given yet.

Part of the difficulty is due to proposed values of $D_{0,1}$, $D_{0,2}$, ΔH_1 , and ΔH_2 not being sufficiently uniquely defined since the fit of two exponentials to the diffusion data is often difficult due to experimental uncertainties and the fact that the curvature, though being pronounced, is observed over an essential part of the accessible temperature range. Sometimes, such a fit is not meaningful at all (e.g. for γ -U) due to the limited temperature range which can be (or happened to be) covered in the experimental investigation.

Such difficulties would be expected to be even more severe for ceramic high temperature materials. Since the temperature of intersection (or "knee temperature") in the Arrhenius diagram is usually quite near to the melting point, such studies should be extended to very high temperatures.

In the following, data on uranium self-diffusion in practically stoichiometric uranium monocarbide, UC, are presented for a broad temperature range. Previous measurements in this system (e.g.2) were performed up to 1900 °C and were fitted to a straight line in the Arrhenius diagram. In the present study, the temperature range is extended up to the melting point, and a curvature of the Arrhenius plot is evident.

This result is discussed in the light of the present knowledge on curved Arrhenius diagrams in various solids.

2. Experimental

Arc cast UC of nearly stoichiometric composition was received from NUKEM, Hanau. Chemical analyses for determining C/U ratios are known to be internally consistent within each laboratory, whereas systematic deviations occur between different laboratories. The analysis of NUKEM yielded 4.81 % C, whereas a series of analyses in the Transuranium gave values

of 4.75 ± 0.02 % C. Therefore, the material was probably as near to stoichiometry (4.80 % C) as one can at present obtain within the U-C system, and was certainly within the range $UC_{1.00 \pm 0.01}$. Analyses were also performed following diffusion anneals since the carbon content in UC tends to increase during prolonged annealing due to preferential evaporation of U-metal (e.g. 3). However, the annealing times were in all cases short enough to not yield a noticeable increase in the C-content. The latter remained always within the range 4.75 to 4.81 %.

The oxygen content was always at the lower limit of detection (100-200 ppm), independent of annealing treatments, and therefore probably predominantly present as oxide layers which are known to form on UC (4). Metallic impurities were ≤ 120 ppm. For diffusion anneals, pellets of 10 mm ϕ and 5 mm height were polished on one face. U-233 was chosen as tracer and deposited by evaporation. Anneals were carried out between 1400 and 2545 °C in a high frequency furnace (5). Two specimens were always annealed in a sandwich-type arrangement with the two coated sides facing one another to minimize disturbing effects of evaporation or chemical attack. Temperatures were measured with a calibrated optical pyrometer. Following the diffusion anneals, the pellets could always be separated (though with some difficulties at the highest temperatures). However, some peak migration was observed at high temperatures, as described previously by one of the authors (5,6) (see also below).

The method of α -energy degradation (7,8) was employed for determining diffusion profiles. In this method, α -spectroscopy using conventional surface-barrier detectors and multi-channel analysers serves to measure energy profiles. These are converted to depth profiles using known values (6) of the energy loss of the α -particles, dE/dx . Diffusion coefficients are then deduced from the concentration vs. depth curves in the usual way.

3. Results

Two typical diffusion profiles are shown in Fig. 1. Following the diffusion anneals, the original line energy spectrum ($t=0$) of the U-233 tracer is extended towards lower energies indicating diffusion of the tracer atoms into the bulk (see Fig. 1, left part). These extended energy spectra can be converted to the desired concentration-depth profiles with the aid of the known energy-depth relation deduced from measurements (6) of dE/dx of the α -particles of U-233 in UC. According to the relevant "thin layer" solution of the diffusion equation

$$C(x,t) = (M/\sqrt{\pi Dt}) \exp (-x^2/4Dt)$$

(with C = concentration of tracer at depth, x , and annealing time, t ; M = total amount of tracer at the surface, $x = 0$, and at $t = 0$; D = diffusion coefficient).

a plot of $\log C$ vs x^2 should give a straight line from the slope of which D can be determined.

Fig. 1 (right part) shows that such straight lines are indeed observed. The small deviations at larger diffusion distances indicate some contribution of fast diffusion paths, e.g. grain boundary diffusion, which, however, was small as would be expected from ceramographic examinations of the diffusion specimens. These showed negligible porosity and a big grain size (up to mm size). A more detailed analysis of grain boundary diffusion in UC will be given later (5).

At higher temperatures, a peak shift as already described in ref. 6 was frequently noted. This was due to some evaporation of the diffusion couples but it was thought to not essentially influence the measured D -values. Again, a more extensive account of the phenomenon will be given elsewhere (5).

A total of 28 experiments was performed in this way, the investigated temperature range being 1480-2545 °C. The resulting diffusion coefficients are shown in an Arrhenius diagram in Fig. 2. They are in addition given in Table I in order to facilitate comparison with the computations given below, where

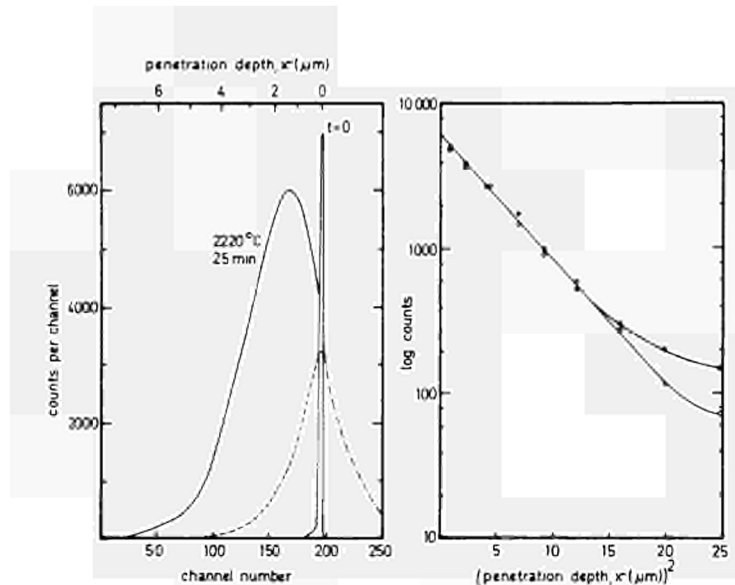


Fig. 1. Extension of α -energy spectra of the initial thin tracer layer of U-233 ($t=0$), on annealing for 25 min at 2220°C (left part). The spectra of the two specimens of the diffusion couple are shown as full or dashed line, respectively. The peak has migrated into one of the specimens by about $1.5\ \mu\text{m}$. The second pellet shows therefore a smaller tracer concentration. The mirror image at the original energy of its spectrum complements the spectrum of the first pellet to a complete Gaussian. This is demonstrated in the right part of the figure by the predominantly straight lines obtained from the two sides of the completed peak in a plot of $\log c$ vs $(\text{depth})^2$. Similar results were obtained at all temperatures.

reference is made to the numbers of the experiments as shown in the last column of Table I. Relevant data points of Lindner, Riemer and Scherff (2) are shown with numbers in brackets in Table I and as open circles in Fig. 2; these were included into the computations since both the experimental techniques and the material used were practically identical in ref. (2) and in the present investigation.

Table I : Diffusion Coefficients for Diffusion of U in UC

Typical result of an interactive computer calculation where, at the start, the first experimental points are attributed to the high temperature process, and the last experimental points to the low temperature process. The calculated D-values for these processes are labelled D-1 and D-2, whereas D stands for the measured coefficients. The values marked with a star have been omitted in some of the calculations (see below).

TEMP	1000/T	D	LOG(D)	D-1	D-2	
2545.	0.3548	0.9200E-10	-10.03633	0.8320E-10	0.9798E-11	1
2525.	0.3573	0.8300E-10	-10.08104	0.6949E-10	0.8807E-11	2
2400.	0.3740	0.2700E-10	-10.56876	0.2122E-10	0.4361E-11	3
2400.	0.3740	0.2000E-10	-10.69910	0.2122E-10	0.4361E-11	4
2330.	0.3841	0.2000E-10	-10.69910	0.1039E-10	0.2857E-11	5
2220.	0.4010	0.7300E-11	-11.13681	0.3120E-11	0.1400E-11	6
2200.	0.4043	0.3200E-11	-11.49499	0.2478E-11	0.1222E-11	7
2200.	0.4043	0.2800E-11	-11.55298	0.2478E-11	0.1222E-11	8
2160.	0.4109	0.2200E-11	-11.65772	0.1546E-11	0.9242E-12	9
2100.	0.4213	0.1600E-11	-11.79602	0.7394E-12	0.5970E-12	10
2000.	0.4399	0.3600E-12	-12.44385	0.1983E-12	0.2738E-12	11
1970.	0.4458	0.3400E-12	-12.46867	0.1306E-12	0.2137E-12	12
1900.	0.4601	0.2800E-12	-12.55299	0.4713E-13	0.1168E-12	(13)
1890.	0.4622	0.2300E-12	-12.63842	0.4052E-13	0.1068E-12	14
1850.	0.4709	0.6800E-13	-13.16765	0.2184E-13	0.7410E-13	15 *
1800.	0.4823	0.7500E-13	-13.12510	0.9751E-14	0.4596E-13	16
1800.	0.4823	0.4000E-13	-13.39810	0.9751E-14	0.4596E-13	17 *
1790.	0.4846	0.7400E-13	-13.13092	0.8260E-14	0.4165E-13	18
1790.	0.4846	0.4800E-13	-13.31892	0.8260E-14	0.4165E-13	19
1780.	0.4870	0.7100E-13	-13.14890	0.6986E-14	0.3772E-13	20
1780.	0.4870	0.4400E-13	-13.35671	0.6986E-14	0.3772E-13	21
1758.	0.4923	0.1100E-12	-12.95876	0.4803E-14	0.3021E-13	(22)*
1700.	0.5068	0.3000E-13	-13.52304	0.1719E-14	0.1644E-13	23
1700.	0.5068	0.1500E-13	-13.82408	0.1719E-14	0.1644E-13	24
1680.	0.5119	0.1200E-13	-13.92099	0.1189E-14	0.1321E-13	25
1680.	0.5119	0.5300E-14	-14.27590	0.1189E-14	0.1321E-13	26 *
1650.	0.5199	0.1200E-13	-13.92099	0.6749E-15	0.9447E-14	(27)
1640.	0.5226	0.3800E-14	-14.42039	0.5564E-15	0.8426E-14	28 *
1495.	0.5655	0.1800E-14	-14.74491	0.2654E-16	0.1389E-14	(29)
1480.	0.5704	0.1800E-14	-14.74491	0.1882E-16	0.1133E-14	30
1480.	0.5704	0.1000E-14	-15.00018	0.1882E-16	0.1133E-14	31
1480.	0.5704	0.5200E-15	-15.28418	0.1882E-16	0.1133E-14	32 *
1400.	0.5976	0.5600E-15	-15.25200	0.2716E-17	0.3600E-15	(33)

Typical experimental errors include an inaccuracy of about $\pm 5^{\circ}\text{C}$ ($T \leq 2000^{\circ}\text{C}$) to $\pm 10^{\circ}\text{C}$ ($T \geq 2000^{\circ}\text{C}$) in temperature measurements, and uncertainties in D of about 10 % in the intermediate temperature range ($1600^{\circ}\text{C} \leq T \leq 2200^{\circ}\text{C}$) whereas both at low temperatures (shallow depth profiles, the depth resolution of the measurements being limited to about $\pm 250 \text{ \AA}$) and high temperatures (short diffusion times due to the fast diffusion), the errors increase to about 20 %.

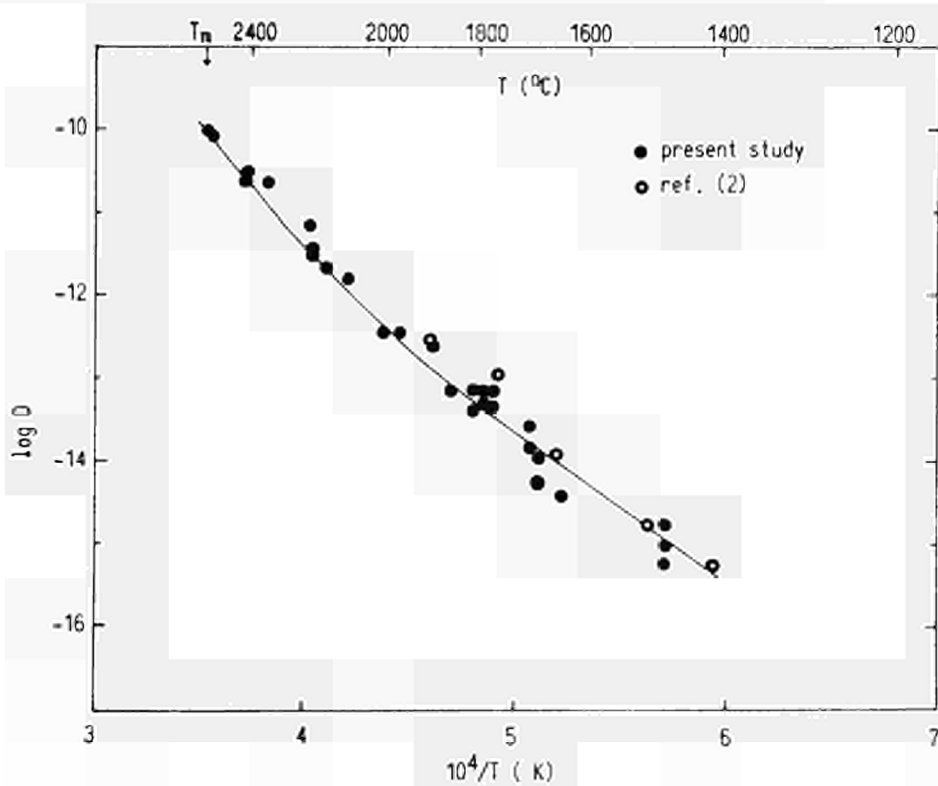


Fig. 2 : Arrhenius plot of the diffusion of U-233 in stoichiometric UC. Data points of Lindner et al. (2) are included as open circles.

Fig. 2 shows clearly a curvature in the Arrhenius plot with a decrease in slope below about 2100°C . The evaluation of Fig. 2 with both a fit with the sum of two exponentials (equ. (2)) and the assumption of two independent processes represented by two straight lines is given in the following Section 4.

4. Evaluation of the non-linear Arrhenius plot.

1. The simplest fit was obtained by arranging the data points according to descending temperatures, and fitting a straight line, by the standard least square fitting procedure, through the logarithm of the diffusion coefficients versus the inverted temperatures, of a lower and higher section of the sequence of data points. Attributing points 1 through 9 (Table I) to the high temperature process only, and points 11 through 33 to the low temperature process only, yields the result :

high temperature process : $\Delta H = 130.2 \pm 9.3$ kcal/mole
" " $\log D_0 = 0.08 \pm 0.78$
low temperature process $\Delta H = 91.3 \pm 5.1$ kcal/mole
" " $\log D_0 = - 3.59 \pm 0.57$
temperature of intersection : 2050°C .

This interpretation should be physically correct for the case where the two independent processes do not occur simultaneously, e.g. if some phase transition occurs around the temperature of intersection.

When both processes do occur simultaneously in the entire range of temperatures studied, however, this procedure will necessarily yield only a crude approximation, except for the extreme case of negligible contribution of the low temperature process to the high temperature section, and vice versa.

The fitting of the sum of two exponentials to the experimental data was attempted in two independent ways :

2. As a first attempt, an iterative fitting procedure was tried. The data points were arranged in order of descending temperature. From this sequence, a high and a low temperature section were taken, initially without overlap. In each section, a straight line was fitted through the logarithm of the difference between the measured diffusion coefficients and the calculated contribution from the other process versus the

inverted temperatures*. The fitting was applied alternatively to either section, until the process converged. The result was then used as a starting approximation for a new series of iterations, in which both the high and the low temperature section were incremented by one data point each, i.e. the next lower or higher point, respectively.

When applied to a synthetic set of data points, (i.e. the calculated sum of two exponentials with known parameters) the input parameters could be retrieved with high precision. When applied to real experimental data, however, the result depended on the choice, which data points were attributed to which section. No asymptotic approach towards some final value appeared with increasing overlap.

As a measure for the quality of the fit, the standard deviation was computed as :

$$\sigma = \left[\sum_{i=1}^n \left\{ \log \left(\frac{D_i}{A_i + B_i} \right) \right\}^2 / (n-2) \right]^{1/2}$$

where D_i stands for each of the n measured diffusion coefficients, and A_i and B_i are the calculated contributions of the high and the low temperature process, respectively, at the same temperature as the corresponding D_i .

With data subjected to experimental errors, σ turned out to be rather insensitive to considerable variations in slopes and intercepts. This means, that a change in one of the parameters could be largely compensated by an adjustment of the remaining parameters. Such an insensitivity of σ has also been observed by other authors (29). Although a selection of the best fit seemed possible by searching for a minimum in σ , the result obtained failed to be convincing. There was no guarantee, that the results of the set of iterations comprised the best fit possible (see also Figs. 5-9).

Fig. 3 shows a plot of the calculated low and high temperature contribution to the Arrhenius Diagram.

* All data points were assumed to have the same relative accuracy. The loss in accuracy on forming the differences was accounted for by weights inversely proportional to the square of the relative error.

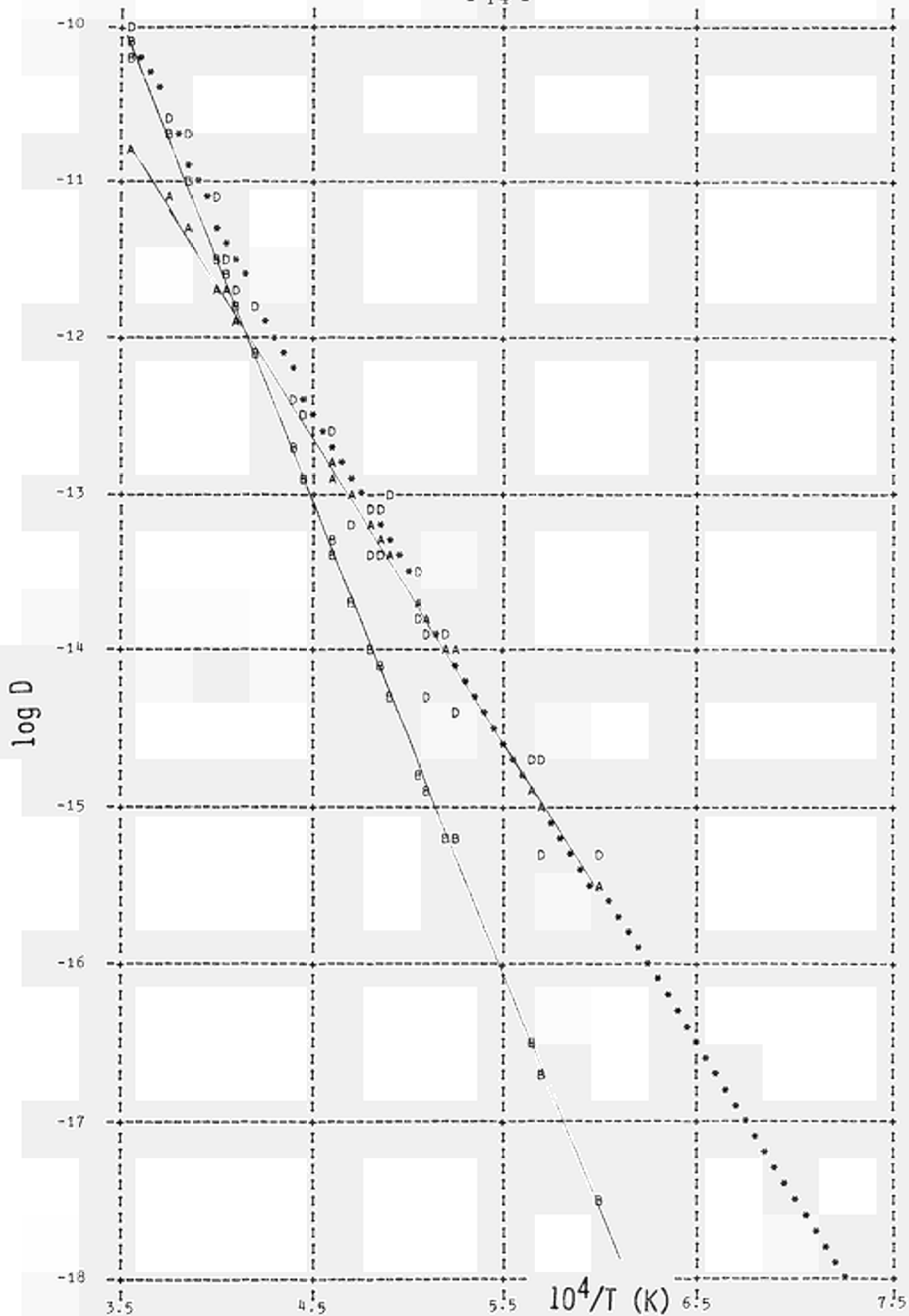


Fig. 3: Computer output of an iterative calculation. The Arrhenius diagram contains the experimental points marked with "D", the calculated low and high temperature processes as "A" and "B". The calculated fit is shown in asterisks.

3. Therefore, it was attempted to minimize σ by varying slopes and intercepts in small steps around the best values obtained so far. This, however, required long calculations. Better results were obtained by variation of one or two parameters in larger steps. Variation of one of the slopes, e.g. ΔH_2 in steps of 1 kcal/mole and adjusting ΔH_1 and both intercepts in order to minimize σ yielded results such as shown in Fig. 4. Adjustment is done by the method of "conjugated gradients" (30). This yields the envelope for possible fits ("one-dimensional scan").

Figs. 5 - 9 show the slopes, intercepts, and calculated intersection temperatures, as a function of the resulting σ , obtained in this way from the 30 best data points. Part of the results of iterative fits are plotted as 'X' in the same figs.

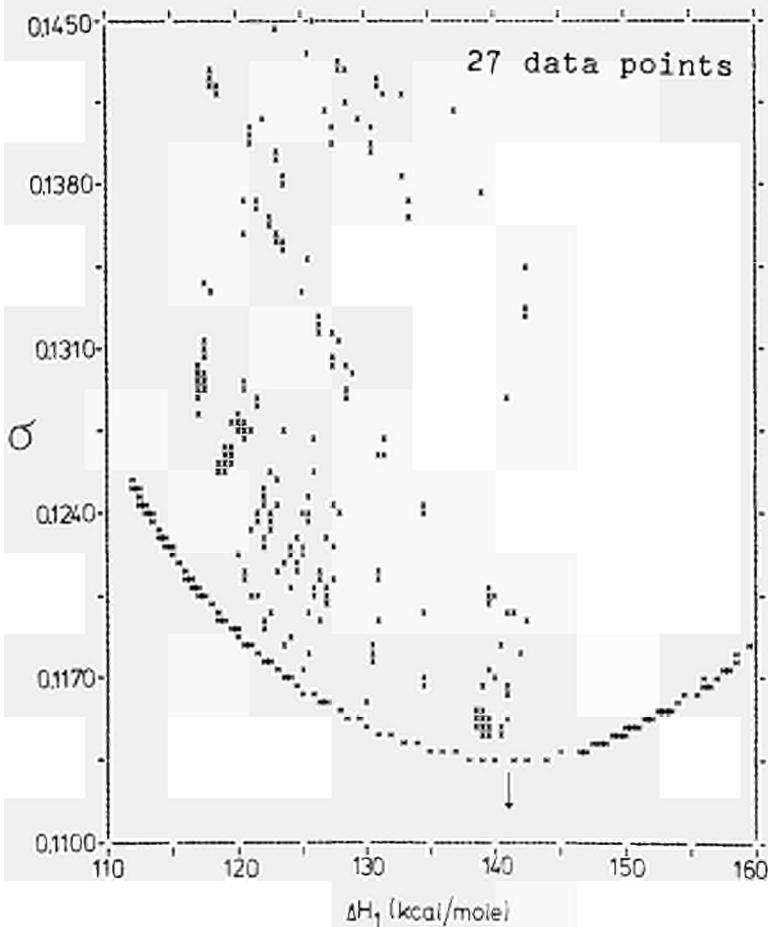


Fig. 4

Plot of the slope of the high temperature process, ΔH_1 , as function of the standard deviation σ . Although the selection of a particular set of results is unique, a relatively small increase in σ may result in a considerable variation of ΔH_1 . Similar plots were obtained for ΔH_2 , $\log D_{0,1}$, $\log D_{0,2}$ and T_{inters} . The envelope, plotted as 'H', was obtained through adjustment with the conjugated gradients method. Results of iterative fits for the same set of data are shown as 'X'.

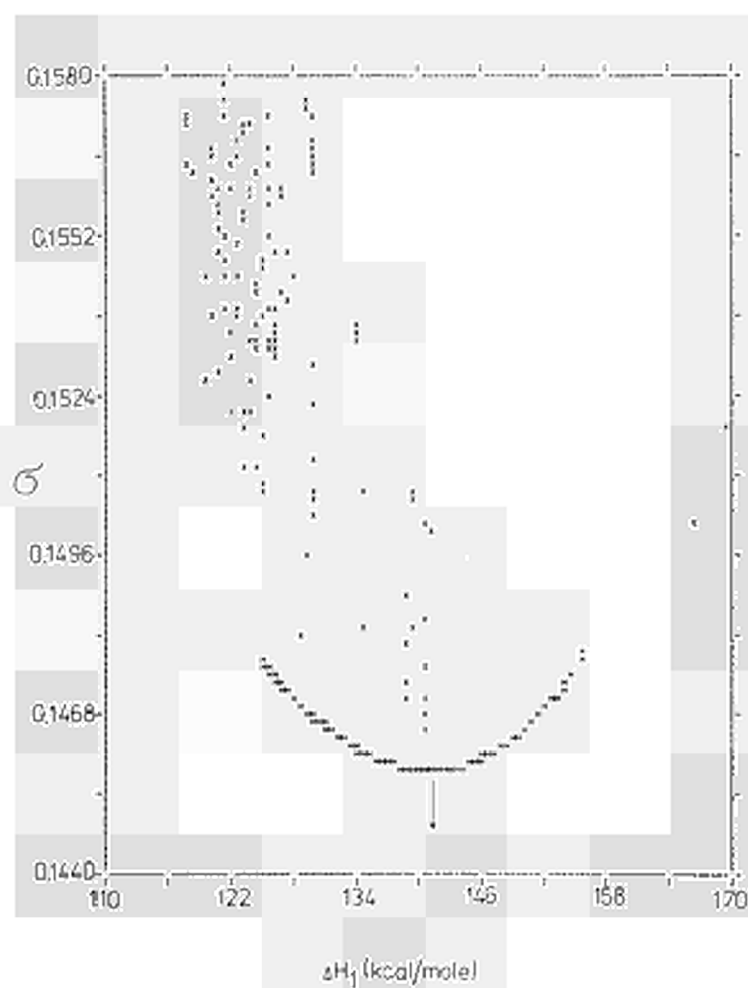


Fig. 5
Plot of ΔH_1 versus σ . The symbols X stand for results of iterative fits.

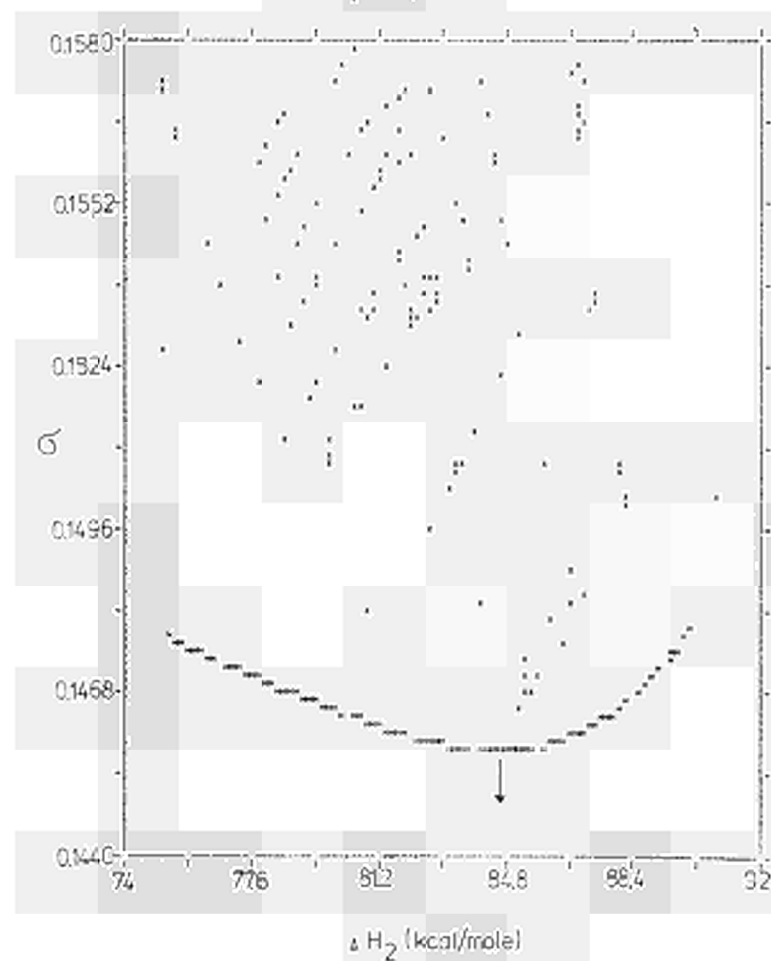


Fig. 6
As above, but for ΔH_2 .

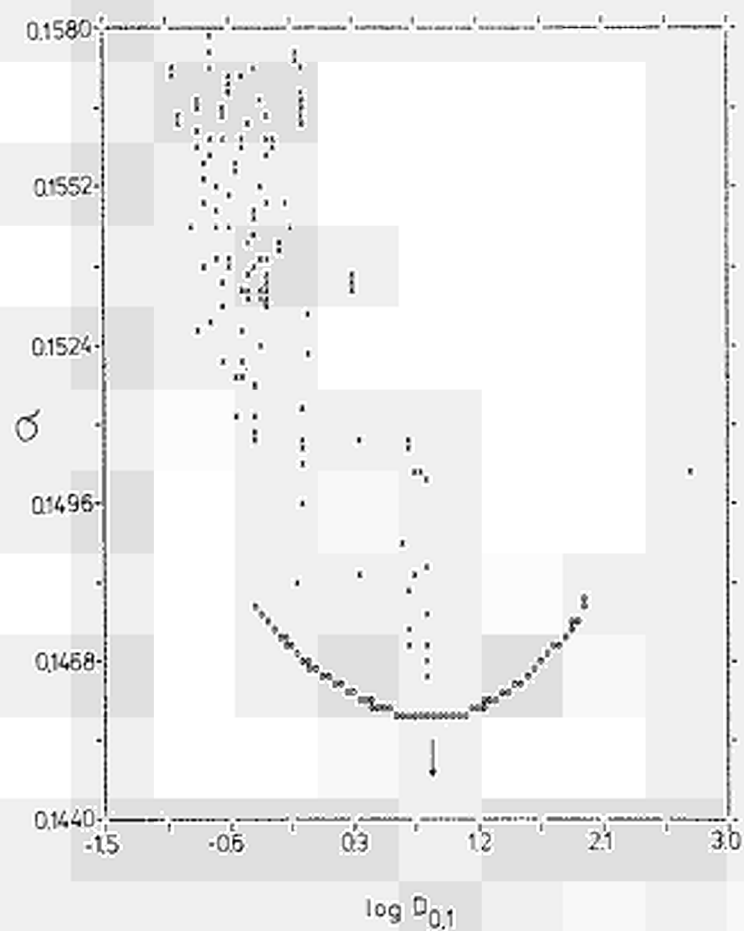


Fig. 7
Plot of $\log D_{0,1}$ versus σ .
The symbols X stand for
results of iterative fits.

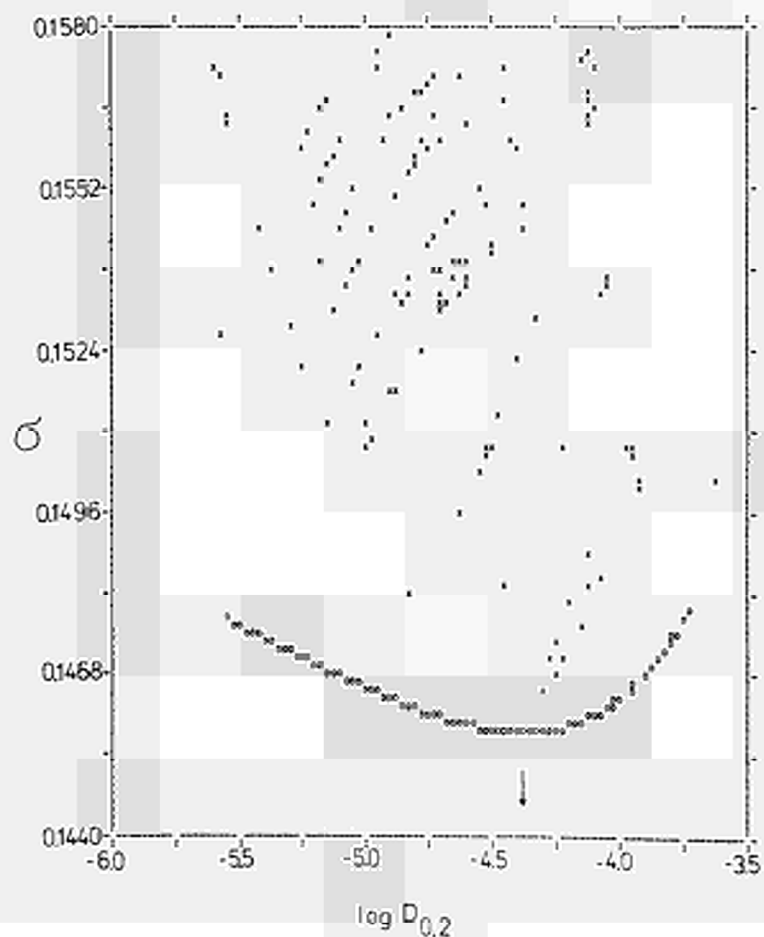


Fig. 8
As above, but for $\log D_{0,2}$.

Variation of both slopes ΔH_1 and ΔH_2 in 1 kcal/mole steps and adjustment of the intercepts in order to minimize σ yielded results such as shown in Figs. 9 - 14 ("two-dimensional scans").

Removing 3 more diffusion coefficients (those which deviated by more than 2σ from the computed curves) did not change the results appreciably, though σ decreased from about 0.14 to about 0.11. Table II summarizes the best fits for 30 and 27 data points. For the latter case, Table III gives an indication of the variation in the parameters with very small changes in σ .

Table II

Calculated diffusion constants for a minimum in the standard deviation and for 27 and 30 experimental points.

	ΔH_1 (kcal/mole)	ΔH_2	$\log D_{o,1}$	$\log D_{o,2}$	$T_{inters.}$ ($^{\circ}C$)
30 points	140.8 \pm 12	84.5 \pm 6	0.83 \pm 1.0	-4.39 \pm 0.8	2083 \pm 40
27 points	141.0 \pm 10	82.8 \pm 4	0.85 \pm 0.8	-4.52 \pm 0.7	2094 \pm 35
suggested data	141 \pm 10	84.0 \pm 5	0.84 \pm 0.9	-4.45 \pm 0.8	2085 \pm 40

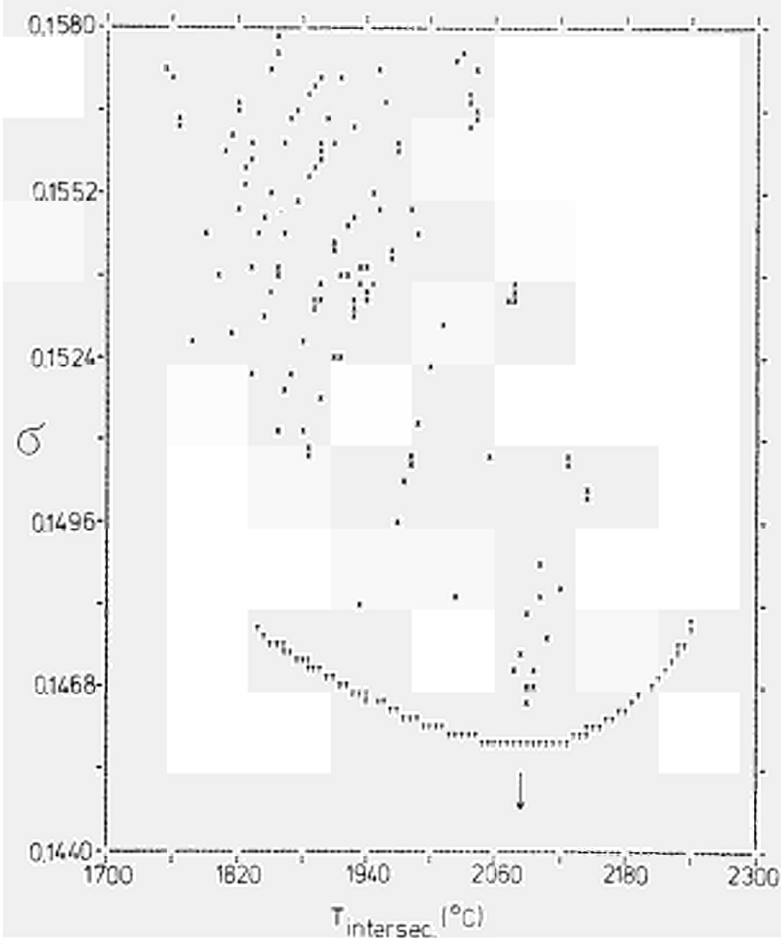


Fig. 9

Plot of the intersection temperature between high and low temperature process, $T_{intersec.}$, versus σ . The symbols X stand for results of iterative fits.

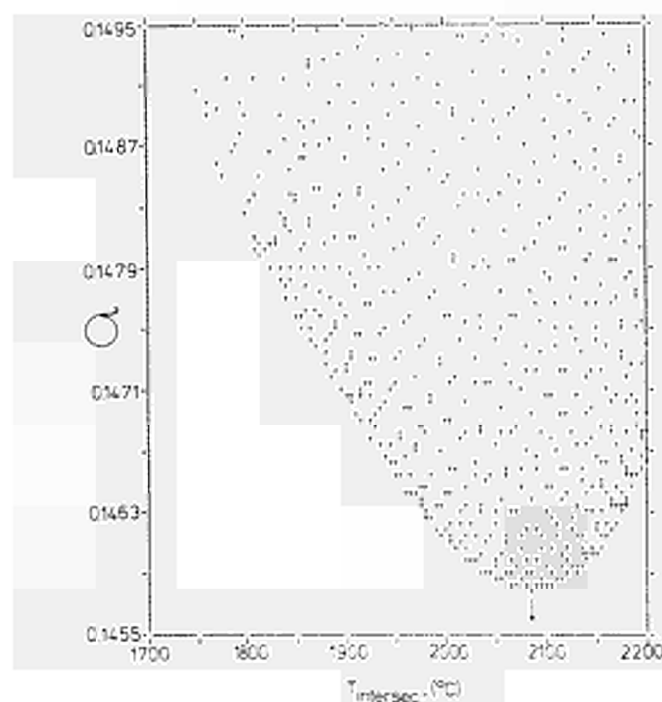
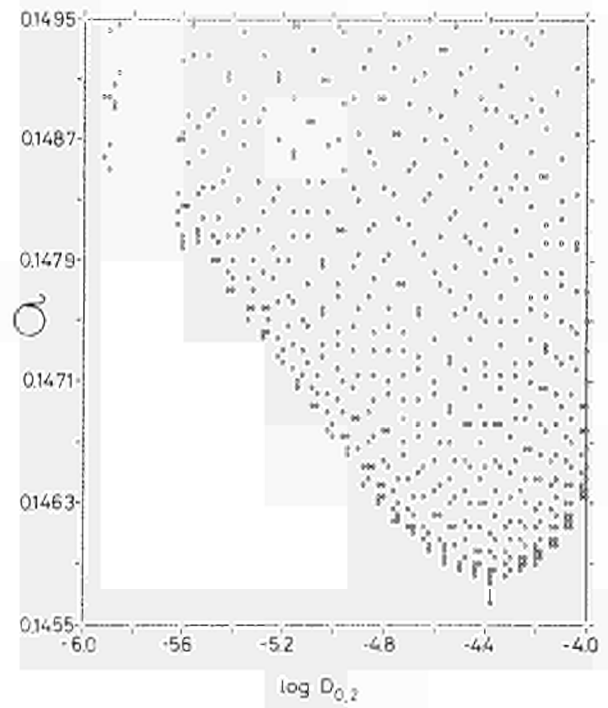
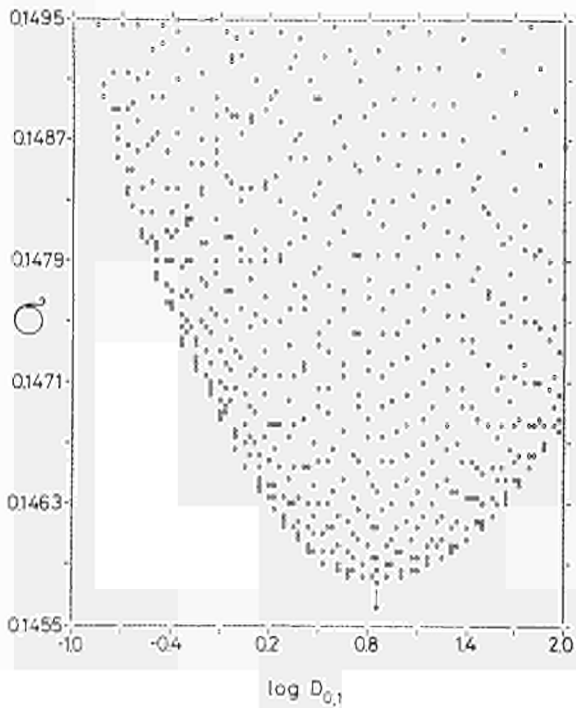
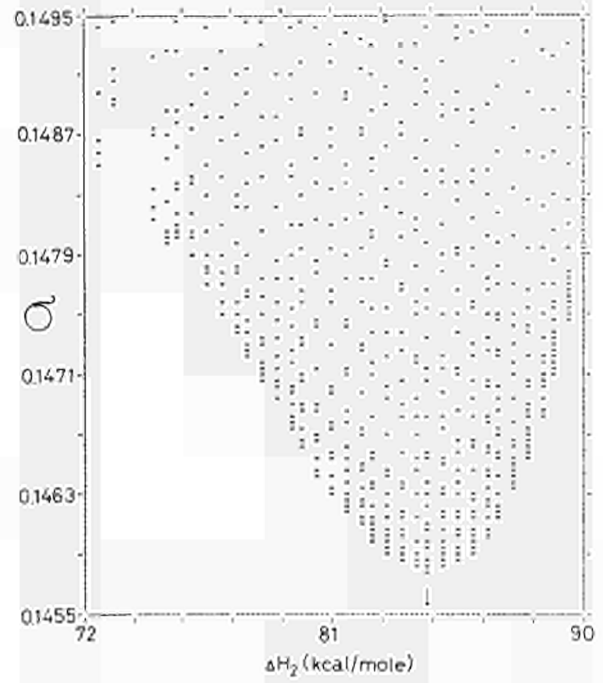
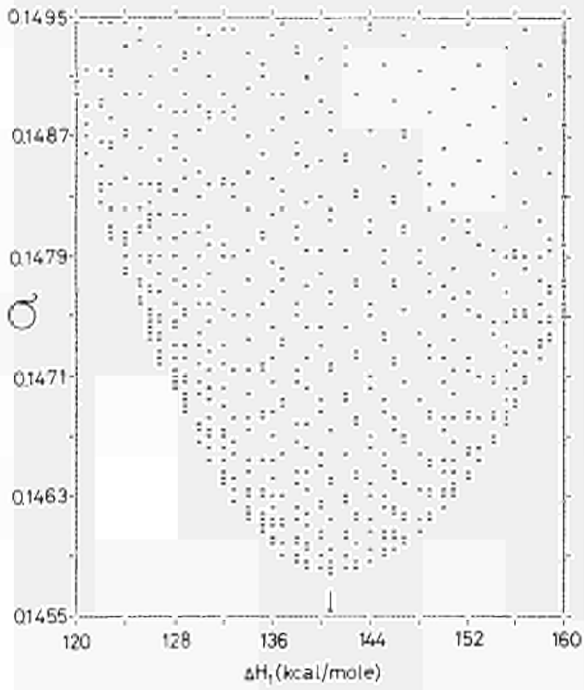


Fig. 10

Plot of $T_{intersec.}$ versus σ for a "two-dimensional scan".



Figs. 11 - 14: Plots of ΔH_1 , ΔH_2 , $\log D_{0,1}$, and $\log D_{0,2}$ versus σ for "two-dimensional scans."

Table III

Calculated fits for the 27 best experimental data points
ordered according to increasing standard
deviation.

σ	ΔH_2	ΔH_1	$\log D_{0,2}$	$\log D_{0,1}$	T_{inters}
0.118043	82.8	140.94	-4.52	0.85	2094
0.118044	83.0	141.42	-4.50	0.88	2100
0.118044	83.0	141.41	-4.50	0.88	2100
0.118047	82.6	140.33	-4.55	0.80	2088
0.118050	83.2	141.90	-4.47	0.92	2105
0.118051	82.5	140.23	-4.56	0.79	2086
0.118055	82.4	139.98	-4.57	0.77	2083
0.118061	83.4	142.39	-4.45	0.96	2111
0.118068	82.2	139.52	-4.59	0.74	2077
0.118068	83.5	142.63	-4.44	0.98	2114
0.118077	83.6	142.88	-4.42	1.00	2117
0.118085	82.0	139.07	-4.62	0.70	2072
0.118086	82.0	139.01	-4.62	0.70	2071
0.118099	83.8	143.38	-4.40	1.04	2122
0.118106	81.8	138.61	-4.64	0.67	2066
0.118127	84.0	143.88	-4.38	1.07	2128
0.118127	84.0	143.88	-4.38	1.07	2128
0.118131	81.6	138.17	-4.67	0.63	2060
0.118145	81.5	137.95	-4.68	0.61	2057
0.118160	81.4	137.73	-4.69	0.60	2055
0.118161	84.2	144.37	-4.35	1.11	2133
0.118192	81.2	137.30	-4.72	0.56	2049
0.118201	84.4	144.90	-4.33	1.15	2139
0.118223	84.5	145.15	-4.32	1.17	2142
0.118227	81.0	136.86	-4.74	0.53	2043
0.118227	81.0	136.87	-4.74	0.53	2043
0.118247	84.6	145.42	-4.31	1.19	2145
0.118265	80.8	136.44	-4.77	0.50	2038
0.118301	84.8	145.93	-4.28	1.23	2150
0.118306	80.6	136.02	-4.79	0.46	2032
0.118328	80.5	135.82	-4.80	0.45	2030
0.118350	80.4	135.60	-4.82	0.43	2027
0.118361	85.0	146.47	-4.26	1.27	2156
0.118361	85.0	146.45	-4.26	1.27	2156
0.118397	80.2	135.20	-4.84	0.40	2021
0.118429	85.2	147.02	-4.23	1.32	2161
0.118446	80.0	134.80	-4.87	0.37	2016
0.118446	80.0	134.80	-4.87	0.37	2016
0.118498	79.8	134.40	-4.89	0.34	2010
0.118504	85.4	147.50	-4.21	1.35	2167
0.118544	85.5	147.80	-4.20	1.38	2170
0.118551	79.6	134.01	-4.92	0.31	2005
0.118579	79.5	133.82	-4.93	0.29	2002
0.118586	85.6	148.03	-4.19	1.39	2172
0.118607	79.4	133.63	-4.94	0.28	1999
0.118665	79.2	133.25	-4.97	0.25	1994

5. Discussion

Before discussing possible reasons for the observed curvature of the Arrhenius plot in uranium self-diffusion in UC, we want to briefly summarize the present knowledge on non-trivial curved Arrhenius plots in various classes of substances. Trivial reasons (see footnote in Introduction) will not be considered nor will all of the original literature references be given. Rather an illustrative selection of typical cases will be presented.

5.1 Summary of Literature Data on Curved Arrhenius Plots

5.1.1. Alkali Halides

The NaCl-type alkali halides are isostructural with UC and will therefore be considered first. In addition, as UC, they consist of two sublattices with different and distinct diffusion properties (though these differences are more pronounced for U and C diffusion in UC than they are for cation and anion diffusion in alkali halides).

A pronounced curvature in the Arrhenius diagrams for anion diffusion was noted for various alkali halides (see Table IV, a and b and summary in ref. (9)). Anion diffusion via divacancies (or vacancy pairs) could in some cases be proven to be the cause for the curvature by performing diffusion runs on doped specimens. Alkali halides heavily doped with a divalent impurity, e.g. Ba^{2+} , have a greatly decreased concentration of single anion vacancies. Therefore, and since the concentration of vacancy pairs is independent of impurity concentration (10), the diffusion via vacancy pairs can be studied selectively. Such measurements showed that the divacancy contribution to self diffusion was more important in causing non-linear Arrhenius plots than the alternative possibility of Coulomb interactions which must exist between vacancies because of their effective charge (e.g. 11) and which were shown to lead to a slight upward curvature of the Arrhenius plot (by 10 to 20 % at T_m). In contrast, a typical

increase due to divacancies is $\geq 100\%$.

The mobility of the vacancy pair is due to a kind of tumbling motion involving mixed sequences of anion and cation jumps with frequencies ν_C and ν_A ; though its mobility contributes to both anion and cation diffusion, these will not necessarily proceed at the same rate. Rather, the ratio of anion to cation diffusion by vacancy pairs is given (12) by

$$D_p^A/D_p^C = \phi' f_p(1/\phi')/f_p(\phi')$$

where A stands for anion, C for cation, and p for pairs, and ϕ' is the ratio of the anion jump frequency to that of the cation jump frequency into the vacancy pair, $\phi' = \nu_A/\nu_C$; $f_p(1/\phi')$ and $f_p(\phi')$ are the correlation factors for anion and cation diffusion via pairs, respectively.

The function $f(\phi')$ has been calculated for NaCl. Therefore, if D_p^A and D_p^C can be measured separately, the ratio of the jump frequencies can be obtained. For NaCl, D_p^A was measured on doped samples and D_p^C was obtained by subtracting the diffusion coefficient calculated from the cation drift mobility in an electric field ($\approx D_v^C$ for single vacancies, since divacancies are neutral and are therefore not affected by an electric field) from the D obtained in tracer diffusion studies ($D = D_v^C + D_p^C$).

In the NaCl-type alkali halides, the anions are less mobile than the cations; the latter, at least in NaCl itself (12), have also the higher diffusion coefficient for vacancy pair diffusion, i.e. the jump rate of cations into vacancy pairs exceeds the jump rate of anions. The opposite seems to be true for the CsCl-type alkali halides. In CsCl, the anions are more mobile, both via single vacancies and via pairs (13), and, so far, a noticeable mobility of cations via divacancies could not be observed in CsCl.

5.1.2. Silver Halides

In silver halides, curved Arrhenius plots were observed in some investigations of both self- and impurity diffusion (e.g. 14,15).

In order to determine the contributing diffusion mechanisms, additional experiments were performed on

- pressure dependence of D
- isotope effect (correlation factor)
- concentration dependence of D (for impurity diffusion)

In brief, the predominant mechanisms could be proven to be a single vacancy mechanism (e.g. Mn in AgBr) or one or two types of interstitialcy mechanism, i.e. a mobility where an interstitial pushes a lattice atom into another interstitial site and jumps into the vacancy created in this way. Such a mechanism can proceed in a collinear or a non-collinear way, depending on temperature, and thus give rise to a curved Arrhenius plot.

5.1.3. fcc Metals

In the close packed metals of the fcc (and hcp) structures, self-diffusion processes show the following features

- a) the Arrhenius plot is straight up to near the melting point, i.e. one diffusion mechanism dominates and both ΔH and D_0 are independent of temperature
- b) the activation enthalpy, ΔH , is approximately $34T_m$ cal/mole, and D_0 is near to unity (range 0.05 to $5 \text{ cm}^2 \text{ sec}^{-1}$)
- c) the data are consistent with a single vacancy diffusion mechanism.

Near to the melting point, however, slight deviations from the Arrhenius law can be detected in high precision measurements, and these can be attributed to divacancy contributions (and possibly a very minor temperature dependence of ΔH). Seeger (1,16) has developed a method for evaluating such small deviations. He introduced five adjustable parameters ($D_{0,1}$; $D_{0,2}$; ΔH_1 ; ΔH_2 ; and α , a coefficient for the possible temperature dependence of the ΔH 's). Since not all five parameters can be determined independently, he suggested to determine functional relationships between the five parameters, hoping that further information (e.g. measurements of the isotope effect or of the pressure dependence of diffusion) may reduce the indeterminacy contained in these functional relationships. Such an evaluation leads to consistent results for the well known metals Ni, Cu, Pt, and Au which are included in Tables IV, a and b. Obviously, the divacancy contributions in fcc metals are small as compared with other

materials showing different diffusion mechanisms and hence curved or composite Arrhenius plots. This is confirmed by the fact that the temperatures of intersection of the two processes would be at or above the melting point (see Table IVb).

5.1.4. "Anomalous" bcc Metals

Some of the bcc metals are called anomalous since diffusion in these metals does not follow the "normal" behavior known from fcc and hcp structures*. These include i) V and Cr, and ii) β -Ti, β -Zr, β -Hf, and γ -U. During the last 10 years, a vast amount of experimental results and speculative interpretations has been accumulated. A conference was devoted to the topic (17) and² recent critical review has been given by Peterson (18). In the following, we will briefly discuss the two types of behavior observed with the "anomalous" bcc metals.

1) For V and Cr, the Arrhenius plots seem to be best represented by two straight lines. For the low temperature region, D_0 and ΔH correspond roughly to what would be expected for a normal metal. Above a critical temperature, T_c , unusually high values of D_0 (10^3 to 10^4 $\text{cm}^2 \text{sec}^{-1}$) and ΔH are observed. For V, $T_c \approx 1700^\circ\text{K}$ or $\approx 0.8 T_m$ (see also Table IV). The abrupt change in diffusion properties at T_c suggests a change in the physical properties of these metals which, however, at present has not been identified. A crystallographic phase change is unprobable but the possibility of an electronic transition (electron transfer between the 3d and 4s states (18)) cannot be excluded. Peart and Askill (19) suggested, based on semiempirical arguments, a single vacancy-divacancy transition at T_c , without, however, explaining the sharp break which was observed instead of the gentle curvature that would normally be expected for such a transition, according to equ. (2). Such a feature is rather observed in the second group of metals.

* Footnote : "Normal" bcc metals include at present Li, Na, K, Fe, Nb, Mo, Ta, and W and show temperature independent values of D_0 and ΔH with a normal range of 0.1 to $10 \text{ cm}^2 \text{sec}^{-1}$ for D_0 and ΔH 's that follow the melting point rule (i.e. $\Delta H \approx 34 T_m \text{ cal/mole}$). With more diffusion studies being performed this classification of the bcc metals may, however, change in future.

Table IVa: Diffusion constants for self-diffusion in substances showing curved Arrhenius diagrams.

Substance	$\log D_{0,1}$	ΔH_1 (eV)	$\log D_{0,2}$	ΔH_2 (eV)	ref.
UC	0.8	6.1	- 4.4	3.7	p.s. a)
UC	0.1	5.7	- 3.6	4.0	p.s. b)
UC _{1.07}	3.0	7.5	- 3.4	4.6	A
KBr	4.5	2.6	-	2.0	BC
KCl	3.9	2.7	1.6	2.1	D
NaBr	-	-	1.7	2.0	E
NaCl(c)	3.0	2.6	0.8	2.0	F-H
LiF(c)	5.6	3.0	1.3	2.1	I
NaF	4.6	3.1	-	2.7	I, J
Ni	0.3	3.24	- 0.3	2.83	K, L
Cu	0.7	2.60	- 0.7	2.09	M
Pt	0.7	3.97	- 0.8	2.87	N
Au	- 0.2	2.37	- 1.4	1.76	O
V	3.4	4.7	- 0.4	3.2	P
Cr	4.0	6.0	0.1	3.5	P
β -Ti	- 0.7	2.4	- 2.8	1.5	P
β -Zr	- 0.5	2.6	- 2.9	1.6	P
β -Hf	-	2.4(d)	- 2.9	1.7	P
γ -U	-	1.9(d)	- 2.8	1.2	P

Index "1" = for high temperature part;

Index "2" = for low temperature part;

p.s. = present study; a) = fitted with the sum of 2 exponentials;

b) fitted with 2 straight lines; c) = average of slightly differing results from different references; d) calculated with the assumption

of $D_{0,1} = 0.2 \text{ cm}^2 \text{ sec}^{-1}$.

Table IVb: Relations for diffusion constants for self-diffusion in substances showing curved Arrhenius diagrams.

Substance	T_m (°K)	$10^3 \Delta H_1 / T_m$ (eV/°K)	$10^3 \Delta H_2 / T_m$ (eV/°K)	$\frac{\Delta H_1}{\Delta H_2}$	$\log D_1^{T_m}$	$\log D_2^{T_m}$	$\log \frac{D_{0,1}}{D_{0,2}}$	T_c (°K)	T_c / T_m
UC ^{a)}	2820	2.2	1.3	1.6	-10.0	-10.9	5.2	2350	0.83
UC ^{b)}	2820	2.0	1.4	1.4	-10.0	-10.7	3.7	2300	0.82
UC _{1.07}	2820	2.7	1.6	1.6	-10.5	-11.6	6.4	2320	0.82
KBr	1002	2.6	2.0	1.3	- 8.5	-	-	-	-
KCl	1048	2.5	2.0	1.3	- 9.0	- 8.4	2.3	>T _m	>1
NaBr	1027	-	2.0	-	-	- 8.2	-	-	-
NaCl	1073	2.4	1.9	1.3	- 8.3	- 8.5	2.2	>T _m	>1
LiF	1142	2.6	1.8	1.4	- 7.6	- 8.0	4.3	1000	0.86
NaF	1260	2.4	2.1	1.2	- 7.7	-	-	<1000	<0.80
Ni	1725	1.88	1.64	1.15	- 8.65	- 8.5	0.6	>T _m	>1
Cu	1355	1.92	1.54	1.24	- 8.9	- 8.5	1.4	>T _m	>1
Pt	2041	1.94	1.41	1.38	- 9.0	- 7.8	1.5	>T _m	>1
Au	1335	1.78	1.32	1.35	- 9.1	- 8.0	1.2	>T _m	>1
V	2160	2.2	1.5	1.5	- 7.5	- 7.9	3.8	1700	0.79
Cr	2160	2.8	1.6	1.7	- 9.9	- 8.2	4.1	1970	0.90
B-Ti	1947	1.2	0.8	1.6	- 6.9	- 6.7	2.1	1620	0.83
B-Zr	2124	1.2	0.8	1.6	- 6.7	- 6.4	2.4	1720	0.80
B-Hf ^{d)}	2420	1.0	0.7	(1.4)	(- 5.7)	- 6.4	(2.2)	(2260)	>0.93
γ-U ^{d)}	1404	1.4	0.9	(1.6)	(- 5.6)	- 7.1	(2.1)	(1320)	>0.92

T_m = melting point (from Handbook of Chemistry and Physics, 51st ed., Chemical Rubber Co, 1970)

D^{T_m} = diffusion coefficient extrapolated to the melting point

T_c = temperature of intersection of high and low temperature process

all other remarks and references as in Table IVa

Comments to Tables IV a,b

The data collected in Tables IVa and b represent partly original data (if one reference only was available), partly averaged values (if different references were available), and partly typical values selected from critical review articles. Citing all of the extensive original literature, especially for the metals, would be beyond the scope of the present discussion. Due to the scatter in experimental results (see e.g. refs. (Q,R) for the scatter for Cr), a few of the listed values for a given material are internally inconsistent (e.g. those for D^m and T_c for Cr). In such cases, data were selected with emphasis on convincingly proven features rather than on numerical extrapolations of reported D_0 and ΔH values.

The typical scatter of the ΔH 's is of the order of $\pm 5\%$, of the D_0 's of a factor of 10, except for the results for fcc metals which are more accurate. Therefore, the ΔH 's etc. for the fcc metals are given with two decimals. Typical uncertainties in $\log D^m$ will be ± 0.5 , in T_c/T_m about ± 0.05 . The data for alkali halides refer to the self-diffusion of the anions, the data for UC are for uranium diffusion.

References to Tables IV a,b

- A) H.J. HIRSCH and H.L. SCHERFF, J. Nucl.Mat. 45 (1973) 123
- B) D.T.DAWSON and L.W. BARR, Proc. Brit. Ceram. Soc. 9 (1967)171
- C) J. ROLFE, Can.J. Phys. 42 (1964)2195
- D) R.G. FULLER, Phys. Rev. 142 (1966)524
- E) H.W. SCHAMP and E. KATZ, Phys.Rev. 94 (1954)828
- F) N. LAURENCE, Phys. Rev. 120 (1960)57
- G) L.W. BARR, J.A. MORRISON, and P.A. Schroeder, J.appl. Phys. 36 (1965)624
- H) M. CHEMLA, Compt.Rend 234(1952)260, and Ann.Phys.1 (1956)959
- I) H.J. MATZKE, J. Phys.Chem. Solids 32 (1971)437
- J) C.F. BAUER and D.H. WHITMORE, phys. stat.sol. 37 (1970)585
- K) A. SEEGER, G. SCHOTTKY, and D.SCHUMACHER, phys.stat.sol. 11 (1965)363
- L) A.SEEGER and D. SCHUMACHER, Mat.Sci.Eng.2 (1967)31
- M) H.MEHRER and A. SEEGER, phys. stat. sol. 35 (1969)313
- N) D.SCHUMACHER, A. SEEGER, and O. HÄRLIN, phys.stat.sol. 25 (1968)359
- O) A.SEEGER and H. MEHRER, phys. stat. sol. 29 (1968)231
- P) R.F. PEART and J. ASKILL, phys.stat.sol. 23 (1967)263
- Q) J. ASKILL and D.H. TOMLIN, Phil. Mag. 11 (1965)467
- R) G.B. FEDOROV, F.I. ZHOMOV, and E.A. SMIRNOV, Met. Metalloved. Chist. Metal. 7 (1968)128.

ii) The group of β -Ti, β -Zr, β -Hf, and γ -U shows continuously curved Arrhenius plots. At low temperatures, the D_0 's are of the order of $10^{-3} \text{ cm}^2 \text{ sec}^{-1}$ and the ΔH 's are about 40 % smaller than would be expected by the melting point rule. Extensive data on impurity diffusion in γ -U and β -Ti (summarized in refs. (17-19)) show the same features as self-diffusion (i.e. $D_{0,1} \approx 1$ and $D_{0,2} \approx 10^{-3} \text{ cm}^2 \text{ sec}^{-1}$ and $\Delta H_1 / \Delta H_2 = 1.8 \pm 0.1$). Attempts have been made to fit the results to the sum of two exponential terms. However, some of the calculated values of $D_{0,1}$, $D_{0,2}$, ΔH_1 and ΔH_2 are not unique due to experimental uncertainties and limited temperature regions for the experiments. The values of $D_{0,1}$ and ΔH_1 (shown in Table IV) would be compatible with expectations for "normal" diffusion in metals, and therefore extensive interpretations were suggested to explain and identify the low temperature contribution to D . These included

- a) grain boundary diffusion which, however, could be excluded with the aid of autoradiography and exact analyses of the penetration profiles.
- b) diffusion along dislocations was shown to be unlikely the only cause for the curvature since otherwise too high a dislocation density would have to be postulated.
- c) any effects of phase changes which occur with these metals between room temperature and the diffusion temperature was shown (20) to be at most small since samples that were pre-annealed at high temperatures for a long time and coated with the tracer at the diffusion temperature showed the same D as did normal specimens, i.e. those coated at room temperature (see, however, also f)).
- d) Kidson (21) and later Le Claire (22) proposed that the curvature of the Arrhenius plot could be due to a strong attraction between vacancies and an impurity in the metal. They showed that the curvature in β -Zr could be accounted for by a low concentration of oxygen atoms in the 10^{-5} range. However, such a mechanism was not supported experimentally, at least for Ti and oxygen as impurity, since diffusion in β -Ti was shown to be identical in high vacuum and in ultra high vacuum.

- e) Peart and Askill (19), based on semi-empirical relations, suggested, in analogy to Cr and V, a vacancy-divacancy mechanism plus a certain contribution of dislocation short-circuits also for the group ii) metals. Seeger and co-workers (1), on the other hand, pointed out that in contrast to fcc metals, divacancies in the bcc structure need a more elaborate treatment, since in the bcc structure there are no lattice sites that are nearest neighbours to both sites of a pair of adjacent sites. This implies that divacancies probably dissociate while moving, that the correlation factor for divacancy diffusion is temperature dependent, etc.. Seeger et al. confirmed the noticeable divacancy contribution in V, and found minor indications of a divacancy mechanism also in the "normal" bcc metals Na, Nb, and Ta.
- f) Seeger (1) suggested also that the low temperature part of the Arrhenius plot might reflect a strong temperature dependence of $D_{0,2}$ and ΔH_2 since the properties (configurations and mobilities) of the vacancies might be affected by the nearness of the phase transition temperature.
- g) There is also the possibility (e.g. 23) that the curvature might be due to a contribution of both nearest-neighbor [111] as well as next-nearest-neighbor [100] single vacancy jumps. These two types of jumps could have different ΔH 's, and such jumps would appear to be more likely for bcc metals than for fcc metals. This suggestion, however, as some of the above ones, fails to explain why the strongly curved Arrhenius plots are observed in some bcc metals only.
- h) Finally, Peterson (18) pointed out that possibly, in analogy to the system Ag/AgBr, a single vacancy - interstitialcy model might be operative with $D_{0,2}$ and ΔH_2 representing the interstitialcy mechanism.

In summary, despite the tremendous effort spent on investigating diffusion processes in bcc metals, the mechanism of diffusion is still very much an open question, and a distinction between vacancy, divacancy, and interstitialcy mechanism cannot safely be made at present.

5.2. Properties of Point Defects in UC

In addition to diffusion studies, measurements of the electrical resistivity of quenched or irradiated specimens are a common tool to investigate properties of point defects. The formation energy of a defect can thus be obtained separately from its migration energy. The former is deduced from the temperature dependence of the quenched-in extra resistivity (which is proportional to the number of frozen-in defects), and the latter can be calculated from the recovery of the electrical resistivity upon subsequent annealing. Diffusion studies yield usually the sum of these two terms. A draw-back of such an indirect type of measurement of resistivity changes lies in the fact that even if a recovery peak is well established, its attribution to a given defect remains frequently a matter of speculation, unless, by analogy to other systems or measurements, a special defect can be attributed unambiguously. Such other measurements might be diffusion studies, where by the choice of the tracer one knows what one is dealing with. Consequently, a combination of the results of both types of studies would be expected to yield confirmatory insights. Therefore, such a combination will be attempted here.

The most recent investigations of quenched, nearly stoichiometric UC have been reported by Schüle et al. (25, 26). By quenching from lower temperatures, 600 to 1070°C, they observed a defect with a formation energy of 1.0 ± 0.1 eV, and a migration energy of roughly 1.45 ± 0.3 eV (annealing peak between 300 and 400°C). The latter value was said to agree with the 1.63 eV deduced from a study (27) of plastic flow and which was attributed to the migration energy of vacancies*.

In this type of study, the migration energy is determined with a smaller accuracy than the formation energy. Since the sum of the two values of 1.0 and 1.45 eV roughly equals reported ΔH 's

* Note, however, that it is difficult to envisage the implied mechanism given the fact that, if at all, the defects with the lower mobility (hence in this case uranium vacancies) should be rate-determining.

for carbon diffusion (see Table V), the observed defects were assumed to be carbon vacancies.

By extending the temperature range of quenching to 1600°C, a new recovery stage above 400°C appeared indicating that another defect had been frozen-in. For this defect, a formation energy of 1.7 ± 0.3 eV and a migration energy roughly in the range of 1.8 to 2.7 eV (possible average 2.2 eV) were determined. Here again, the second of these values is much less accurate. Since the sum of 1.7 and 2.2 eV equals published values of uranium diffusion (see Table V), the observed defects were suggested to be uranium vacancies. These values were supported by a re-interpretation of previous quenching data (24, 25). Following neutron irradiation (28, 31 - 34), three more recovery peaks (at 150, 500, and 800°C) are observed. Their interpretation seems less clear; the first peak could be due to (uranium ?) interstitials, since interstitial atoms have been reported to migrate in UC at and near room temperature (36). A consistent picture for all features observed so far is, however, still missing.

These results, together with the deductions of Section 5.1, will be used to discuss possible mechanisms that might explain the observed curvature in the Arrhenius diagram for uranium diffusion in UC.

5.3. Possible Divacancy Contribution to Uranium Self-Diffusion in UC

It is tempting to attribute the curvature in the Arrhenius-plot to a predominant single vacancy mechanism at low temperatures, and a predominant divacancy mechanism at high temperatures. A number of arguments in favor for this mechanism can be cited based on the existing knowledge summarized in the two preceding sections.

These arguments include

- a) Divacancies contribute appreciably to self-diffusion in
the isostructural

alkali halides. As shown in Table IV b, both the ratio's of $\Delta H_1/\Delta H_2$ (of about 1.4 ± 0.2) and the relative temperatures of intersection of the high and the low temperature process ($0.8 T_m$) are similar for these two classes of materials.

- b) The present value of ΔH_2 for the low temperature process of 3.7 eV is in good agreement with the sum of 1.7 and 2.2 eV, values which have been reported (see Section 5.2) for the formation and migration energies of single uranium vacancies, respectively, in studies of electrical resistivity using quenched samples.
- c) This value of 3.7 eV for ΔH_2 follows reasonably well the melting point rule for single vacancy diffusion (in normal metals), i.e. $\Delta H \approx 34 T_m$ cal/mole. (The present ΔH_2 can be represented by $\Delta H_2^{UC^m} = 30 T_m$ cal/mole)
- d) It is in addition reasonable with regard to a further empirical rule (44) relating self diffusion with rare gas diffusion. The latter can normally be measured quite accurately since it is usually not perturbed by impurities or imperfections. According to this rule, ($\Delta H_{\text{gas}} = (0.86 \pm 0.10) \Delta H_{\text{self diff}}$) a ΔH in the range of 3.8 to 4.8 eV would be expected, which is not too far from the reported value (though the latter appears to be on the low side).

All this reasoning is in favor of a divacancy diffusion mechanism at high temperatures. If such a mechanism is really operative, it should have a ΔH given by

$$\Delta H_D^{2v} = 2 \Delta H_F^{1v} + \Delta H_M^{2v} - B^{2v}$$

where $\Delta H_D^{2v} = \Delta H_1$ with $2v$ standing for divacancies and D for diffusion. Similarly, $1v$ stands for single vacancies, F for the formation and M for the migration term, and B^{2v} for the binding energy of divacancies. In the present case, and with $\Delta H_F^{1v} = 1.7$ eV (see Section 5.2.), we would have

$$6.1 \text{ eV} = 3.4 \text{ eV} + (\Delta H_M^{2v} - B^{2v}).$$

The binding energy of divacancies is usually quite small. B^{2v} is known for metals (e.g. Ni, Pt, and Au) where it varies between 0.1 to 0.3 eV. Therefore, the migration energy of the

divacancy would be

$$\Delta H_M^{2v} \approx 3 \text{ eV}$$

hence it would be slightly bigger than the reported range for ΔH_M^{1v} of up to 2.8 eV (see Section 5.2.). In metals, normally the reverse is true. Moreover, the properties of carbides are sufficiently different from those of metals to avoid stressing any analogy too far.

There are, however, arguments that seem to be less compatible with the single vacancy-divacancy mechanism. These include

- a) The D_0 for the low temperature process ($D_{0,2} = 3.6 \times 10^{-5} \text{ cm}^2 \text{ sec}^{-1}$) is very low. "Normal" values for a single vacancy mechanism center around $10^{0+1} \text{ cm}^2 \text{ sec}^{-1}$.
- b) Accordingly, the D_0 for the high temperature process ($D_{0,1} = 6.9 \text{ cm}^2 \text{ sec}^{-1}$) is much smaller than most literature values for divacancies. It rather coincides with the expectation for a single vacancy mechanism.

A final decision on the suggested divacancy mechanism could in principle be made once additional independent experimental evidence becomes available. Such evidence could be

- i) measurement of the isotope effect. Such measurements, however, seem unfeasible for UC due to the small mass differences between the available uranium tracer isotopes and the high temperatures needed.
- ii) measurement of the pressure dependence of D . This again would not be thought to be promising for a ceramic and experimental temperatures in excess of 2000°C .

Therefore, a final decision would probably have to wait until more knowledge on mass transport processes in carbides is available. At present, the single vacancy-divacancy mechanism seems to be favored. Other possible alternatives are discussed in the following section.

6. Conclusions and Summary

The decomposition of a curved Arrhenius diagram is a difficult task. Previous authors (29) have stated that if the analysis is to be precise, one of the exponents should be at least twice

the other. Even for such a favorable case, a computer fitting shows that the parameters can still vary considerably, even if the standard deviation has (or appears to have) reached a minimum.

Table V

Relevant self-diffusion studies in near stoichiometric UC

Tracer	C / U ratio	ΔH (eV)	$\log D_0$	T-range ($^{\circ}C$)	ref
U	1.006	3.9	-3.7	1400-1900	2
U	0.973	3.0	-5.2	1600-2100	2
U	0.96-1.04	≈ 3.5	-4.1	1600-2000	37
U	1.0	3.7	-4.4	1400-2085	p.s.
C	1.004	2.7	0.2	1300-1700	41
C	0.98	3.9	1.5	1450-1800	41
C	0.98-1.01	2.7	-1.0	900-1500	42
C	0.96-1.00	3.6-4.1	-	1500-1900	38
C	0.96-1.00	2.2-2.3	-	1150-1500	38
C	1.0	2.8	-0.5	1185-2350	43

p.s. = present study

The results on U-diffusion of refs. (38-41) were omitted since they yield values which are by far too high. A discussion of these data will be given elsewhere (5).

In the present study, a procedure was therefore developed which is thought to yield reliable data, at least in not too unfavorable cases (essential scatter of the experimental data points and/or similar values of ΔH_1 and ΔH_2). With iterative fits, probable sets of ΔH_1 , ΔH_2 , $D_{0,1}$ and $D_{0,2}$ are calculated. Subsequently, one or two of the parameters are stepwise varied around the probable result, and the remaining parameters are adjusted in order to minimize the standard deviation. This yields an envelope for possible fits from which the most probable set of the four parameters can be selected.

This procedure yielded the following results for the observed curved Arrhenius plot for uranium diffusion in stoichiometric UC

at high temperatures $\Delta H_1 = 6.1$ eV and $D_{0,1} = 6.9$ cm²sec⁻¹
at low temperatures $\Delta H_2 = 3.7$ eV and $D_{1,2} = 3.6 \times 10^{-5}$ cm²sec⁻¹

A fit of two straight lines to the curved Arrhenius plot resulted in the set of values

$$\Delta H_1 = 5.7 \text{ eV and } D_{0,1} = 1.2 \text{ cm}^2 \text{ sec}^{-1}$$
$$\Delta H_2 = 4.0 \text{ eV and } D_{0,2} = 2.5 \times 10^{-4} \text{ cm}^2 \text{ sec}^{-1}$$

The latter fit would be physically meaningful, if a phase changes would occur at the intersection temperature. The presently accepted phase diagram of the U-C system (e.g. 3), however, predicts a range of solid solubility between UC_{0.9} and UC_{1.1} at 2000°C. Therefore, the former fit with the sum of two exponentials seems to be the only realistic one.

Arguments in favor of a predominant divacancy mechanism above 2085°C and a predominant single vacancy mechanism below this temperature have been given in Section 5.3. Possible alternatives to this mechanism, i.e. a single vacancy mechanism above 2085°C and a second mechanism at lower temperatures, will be discussed in the following. For the low temperature process,

- grain boundary diffusion can safely be discarded on basis of autoradiography. In addition, most diffusion specimens consisted of a few grains only.
- fast diffusion along dislocations as only cause would necessitate a dislocation density which would be unlikely high for a ceramic
- effects of impurities seem to be the most likely alternative to a divacancy-vacancy mechanism. Both oxygen which is known to exist as U(C,O)-phases, as well as metallic impurities (W, but also Fe, Cr, Ni) could cause the observed curvature in the Arrhenius-diagram due to strong attractions between vacancies and impurities. Experiments on very pure

UC, or a thorough study on the effect of the above impurities on uranium self-diffusion could settle this question. Alternative means would be to measure the isotope effect and the effect of pressure on uranium self-diffusion.

A further reason for a curved Arrhenius diagram would be a temperature dependence of ΔH . This possibility, however, is unlikely since any temperature dependences of ΔH 's postulated in diffusion work so far were at the most very small. An increase in ΔH of nearly 70 % at the melting point, as observed here for UC, would certainly not be expected for a temperature dependent ΔH .

The low temperature part observed here compares favorably with reliable literature data (see Table). None of the literature studies was extended to high enough temperatures to observe the curvature in the Arrhenius plot. The high temperature part reported here has therefore no analog in literature.

References

- 1) A. SEEGER, J. Less-Common Metals 28 (1972)387
- 2) R. LINDNER, G. RIEMER, and H.L. SCHERFF, J. Nucl.Mat. 23 (1967)222
- 3) E.K. STORMS, "The Refractory Carbides", Academic Press, New York (1967)
- 4) Hj. MATZKE, J. Appl. Phys. 40 (1969)3819
- 5) Hj. MATZKE, to be published
- 6) H.J. HIRSCH and Hj. MATZKE, J. Nucl. Mat. 45 (1972/73)29
- 7) F. SCHMITZ and R.LINDNER, J. Nucl. Mat 17(1965)259
- 8) F. SCHMITZ, PhD-THESIS, Technical University Braunschweig (1965)
- 9) Hj. MATZKE, J. Phys.Chem. Solids 32 (1971)437
- 10) e.g. A.B. LIDIARD, in Handbuch der Physik 20 (1970)246, Springer, Berlin
- 11) S. CHANDRA and J. ROLFE, Can.J.Phys. 48(1970)397 and 412
- 12) V.C. NELSON and R.J. FRIAUF, J. Phys.Chem.Solids 31 (1970) 825
- 13) I.M.HOODLESS and R.G. TURNER, J. Phys.Chem. Solids 33(1972)1915
- 14) P.SÜPTITZ and J. TELTOW, phys.stat.sol. 23 (1967)9
- 15) P.SÜPTITZ, in Reactivity of Solids, p. 29, Eds.J.W.MITCHELL, R.C. de VRIES, R.W. ROBERTS, and P. CANNON, Wiley-Inter-science, New York (1968)
- 16) A. SEEGER, Comments on Solid State Physics 4 (1971)19
- 17) Diffusion in Body-Centered Cubic Metals, Amer.Soc.Metals, Champman and Hall, London (1965)
- 18) N.L. PETERSON, Diffusion in Metals, in F. SEITZ, D.TURBULL, and H. EHRENREICH (eds.) Solid State Physics, Vol 22, Academic Press, New York (1968)
- 19) R.F. PEART and J. ASKILL, phys.stat.sol. 23 (1967)263
- 20) N.L. PETERSON and S.J.ROTHMAN, Phys.Rev. 136 (1964)842
- 21) G.V. KIDSON, Can.J.Phys. 41(1963)1563
- 22) A.D. LE CLAIRE, in ref. (17), p.3
- 23) M.S. WECHSLER, in ref. (17), p.375
- 24) L.B. GRIFFITHS,Phil.Mag. 7 (1962)827
- 25) W.SCHÜLE and P. SPINDLER, J. Nucl.Mat. 32 (1969)20
- 26) D. DONNER and W. SCHÜLE, J. Nucl.Mat. 45(1972) in press
- 27) R.CHANG, J. Appl. Phys. 33 (1962)858
- 28) B.G. CHILDS and J.C. RUCKMAN in New Nuclear Materials, Including Non-Metallic Fuels, IAEA Vienna 2 (1963)1

- 29) L.W. Barr and A.B. Lidiard, Phys.Chemistry - An Advanced Treatise, Vol. 10, Academic Press (1969)
- 30) R. Fletcher and C.M. Reeves, Computer Journal 7(1964)149
- 31) B.G. Childs, A. Ogilvie, J.C. Ruckman, and J. L. Whitton, Symp. Rad. Damage in Solids and Reactor Materials, IAEA, 4 (1963) 241
- 32) B.G. Childs, J.C. Ruckman, and K. Buxton, Carbides in Nuclear Energy 2 (1964) 869
- 33) L.B. Griffiths, J.Nucl.Mat. 4 (1961) 336
- 34) J. Bloch and J.P. Mustelier, J.Nucl.Mat. 17 (1965) 350
- 35) H. Matsui and T. Kirihara, J.Nucl.Sci.Techn.9 (1972)618
- 36) Hj. Matzke, Solid State Comm. 7 (1969) 549
- 37) P. Villaine and J.F. Marin, CR Acad. Sc. Paris 264 c (1967) 2015
- 38) G.G. Bentle and G. Ervin, Jr; US report AI-AEC 12726 (1968)
- 39) F.A. Rough and W. Chubb, US Report BMI-1488 (1960)
- 40) W.Chubb, R.W. Getz, and C.W. Townley, J. Nucl. Mat. 13 (1964) 63
- 41) H.M. Lee and L.R. Barrett, Proc. Brit. Ceram. Soc. 7 (1967) 159, and J. Nucl.Mat. 27 (1968) 275
- 42) R.A. Krakowski, J. Nucl.Mat. 32 (1969) 120
- 43) T.C. Wallace, W.G. Witteman, C.L. Radosevich, and M.G. Bowman, US Report LA-DC 8840 (1968)
- 44) Hj. Matzke, Physics of Ionized Gases, Ed. B. Navinsek, Ljubljana (1970) p. 326

Appendix

In the following Appendix, typical literature results on curved Arrhenius plots will be reanalyzed using the present computer programs (see Section 4). The data are due to

- 1) H.J. Hirsch and H.L. Scherff, J.Nucl.Mat.45 (1973)123:
Uranium Diffusion in hyperstoichiometric uranium monocarbide, UC_{1.07}
- 2) D.K. Dawson and L.W. Barr, Proc.Brit.Ceram.Soc.9 (1967)171:
Diffusion of Br in KBr.
- 3) J.F. Murdock, T.S.Lundy, and E.E.Stansbury, Acta Met.12 (1964)1033: Diffusion of Ti and V in Ti.

These examples represent high accuracy results with a scatter that is less than average. It is therefore instructive to realize that nevertheless essential changes in the calculated diffusion parameters can be obtained if an - on first sight apparently small-increase in the standard deviation σ of 10^{-3} is allowed. Such an increase in σ can cause maximum changes between the calculated highest and lowest values of ΔH_1 and ΔH_2 as follows

	maximum change in %	
	ΔH_1	ΔH_2
U/UC _{1.07}	7	8
Br/KBr	6	6
Ti/Ti	>20	>30
V/Ti	12	80

The data and the calculated fits are discussed in more detail in the following.

1) Uranium diffusion in $UC_{1.07}$ by Hirsch and Scherff

These data were selected because of their relevance to the present study. The authors suggest that two independent processes occur above and below $2050^{\circ}C$ due to crossing the phase boundary between a two-phase region ($UC + UC_2$ for $T < 2050^{\circ}C$) and a single phase region (UC_{1+x} for $T > 2050^{\circ}C$). They suggest further that the phase diagram of the U-C system be revised, since the previously accepted phase diagram indicates this boundary to be at essentially lower temperatures of $\approx 1800^{\circ}C$. They nevertheless give also an evaluation in terms of the sum of two exponentials.

Fig. 15 shows that the data should be well suitable for evaluation since the low and high temperature parts are essentially different with a ratio in slope of about a factor of 2.

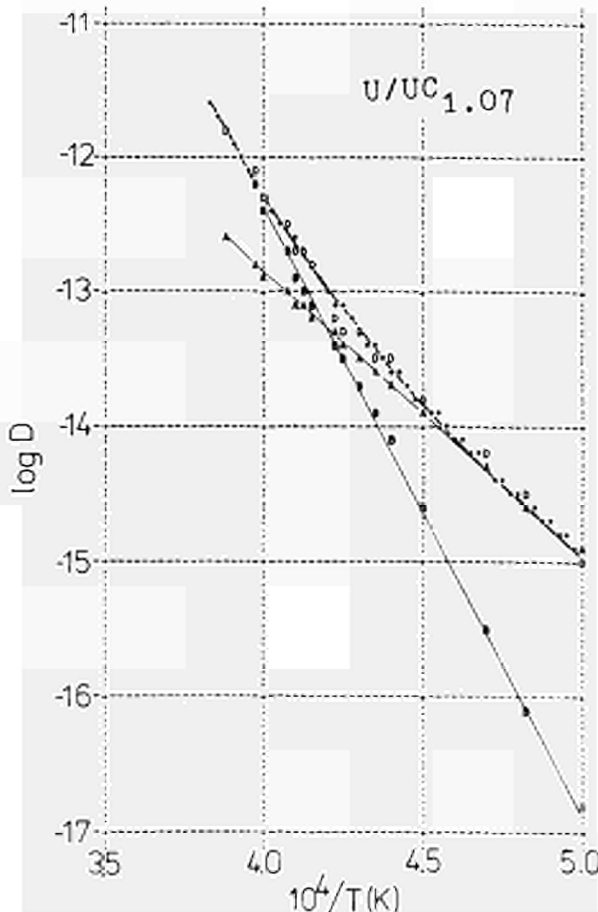


Fig. 15

Computer output of an iterative fit. The Arrhenius diagram contains the experimental points marked with "D", and the calculated low and high temperature processes as "A" and "B", respectively. The calculated fit is shown in asterisks.

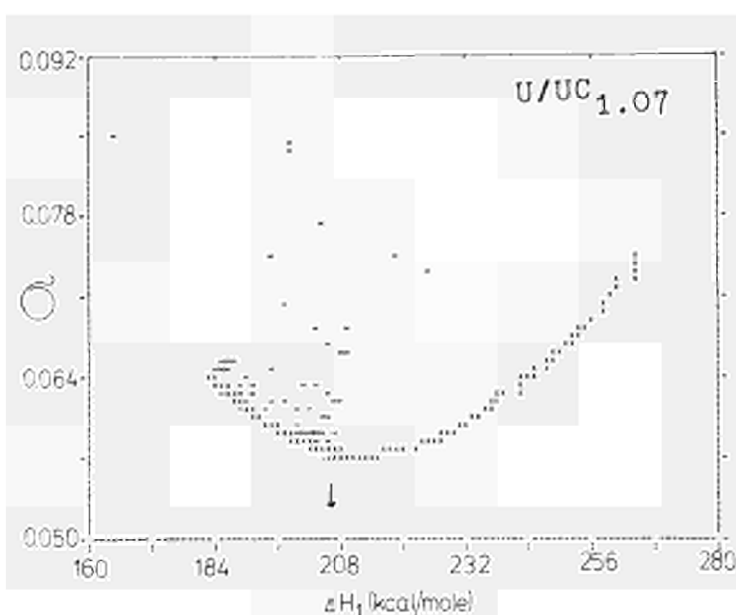


Fig. 16

Plot of ΔH_1 versus σ for a "one-dimensional scan". The symbols X stand for iterative fits.

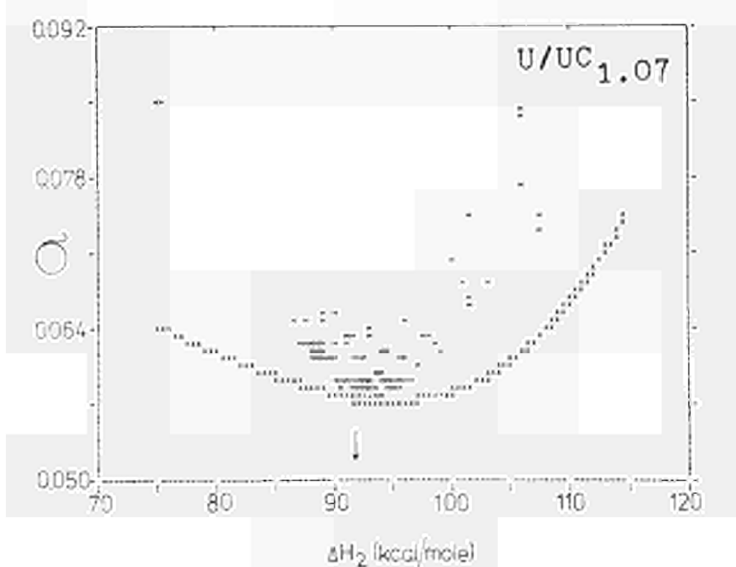


Fig. 17

As above, but for ΔH_2

Further calculated fits are given in Table VI. The best fit was obtained with the following set of data

	ΔH_1	ΔH_2	$\log D_{0,1}$	$\log D_{0,2}$	$T_{inters.}$
	(kcal/mole)				(°C)
present values	204.9	91.7	5.5	-4.9	2093
authors' values	200	90	-	-	-

Table VI

Calculated fits to the data of Hirsch and Scherff ordered according to increasing standard deviation.

σ	ΔH_2	ΔH_1	$\log D_{0,2}$	$\log D_{0,1}$	T_{inters}
00.005774	91.67	204.85	-4.91	5.54	2093
00.005788	93.47	205.58	-4.72	5.59	2101
00.005801	94.05	205.76	-4.66	5.60	2104
00.005809	94.30	205.84	-4.63	5.61	2105
00.005815	94.32	205.87	-4.63	5.61	2105
00.005835	90.60	200.42	-5.02	5.16	2082
00.005836	91.60	201.21	-4.92	5.22	2087
00.005841	92.28	201.75	-4.84	5.26	2091
00.005843	95.02	206.06	-4.55	5.62	2109
00.005844	91.45	200.69	-4.93	5.18	2086
00.005847	92.19	201.42	-4.86	5.24	2090
00.005848	90.42	199.65	-5.04	5.09	2080
00.005850	92.88	202.19	-4.78	5.30	2094
00.005852	92.83	202.04	-4.79	5.29	2093
00.005858	93.28	202.49	-4.74	5.32	2096
00.005858	93.22	202.47	-4.74	5.32	2096
00.005862	93.42	202.71	-4.72	5.34	2097
00.005863	93.40	202.64	-4.73	5.34	2097
00.005866	95.63	206.17	-4.49	5.63	2111
00.005872	95.75	206.19	-4.48	5.63	2111
00.005876	91.68	199.68	-4.91	5.09	2085
00.005877	92.36	200.46	-4.84	5.15	2089
00.005878	90.95	198.80	-4.99	5.01	2081
00.005881	92.88	201.08	-4.78	5.20	2092
00.005883	93.06	201.42	-4.76	5.23	2094
00.005885	94.41	203.63	-4.62	5.42	2102
00.005887	89.95	197.61	-5.09	4.91	2075
00.005891	94.33	203.29	-4.63	5.39	2102
00.005896	94.89	203.89	-4.57	5.44	2104
00.005900	90.72	198.23	-5.01	4.97	2078
00.005900	89.83	197.22	-5.11	4.88	2074
00.005901	95.04	204.01	-4.55	5.45	2105
00.005901	94.19	202.72	-4.64	5.34	2100
00.005902	94.77	203.47	-4.58	5.40	2103
00.005904	90.64	197.80	-5.02	4.93	2078
00.005908	96.34	206.29	-4.42	5.64	2114
00.005908	94.91	203.55	-4.57	5.41	2104
00.005909	91.18	198.19	-4.96	4.96	2080
00.005909	94.64	202.99	-4.60	5.36	2102
00.005910	91.19	198.41	-4.96	4.98	2081
00.005914	94.82	203.18	-4.58	5.38	2103
00.005917	91.70	198.54	-4.91	4.99	2083
00.005921	91.63	198.57	-4.92	4.99	2083
00.005927	92.19	198.88	-4.86	5.02	2086
00.005930	95.79	204.62	-4.48	5.50	2109
00.005932	92.33	199.03	-4.84	5.03	2087
00.005933	92.08	198.73	-4.87	5.00	2085
00.005936	95.64	204.02	-4.49	5.45	2108
00.005940	95.62	203.97	-4.49	5.44	2107
00.005944	92.21	198.80	-4.86	5.01	2086
00.005964	93.39	199.76	-4.73	5.09	2092
00.005968	93.65	199.83	-4.70	5.09	2093
00.005975	93.82	199.94	-4.69	5.10	2094
00.005986	93.33	199.14	-4.74	5.03	2090
00.005993	93.47	199.19	-4.72	5.04	2091
00.006021	97.08	205.97	-4.34	5.61	2118
00.006021	97.08	205.98	-4.34	5.61	2118
00.006038	96.79	204.85	-4.37	5.51	2115
00.006099	95.84	201.44	-4.47	5.22	2106
00.006106	90.09	191.59	-5.09	4.39	2066

2. Bromine diffusion in KBr by Dawson and Barr

These data were selected because of the clear separation of high and low temperature part and because of the accuracy of the results (see also Fig. 18). The authors suggest a vacancy mechanism of diffusion at high temperatures and a fast diffusion along dislocations at low temperatures.

Due to the nature of the data, the minima in the one-dimensional fits are very pronounced for all 5 quantities (ΔH_1 , ΔH_2 , $\log D_{0,1}$, $\log D_{0,2}$, and T_{inters} ; see also Figs. 19, 20). The best fit was obtained with the following set of data

	ΔH_1	ΔH_2	$\log D_{0,1}$	$\log D_{0,2}$	T_{inters}
	(kcal/mole)				
present values	70.5	36.0	6.5	-1.9	600 °C
authors' values	60.0	34.3	3.5	-2.5	520 °C

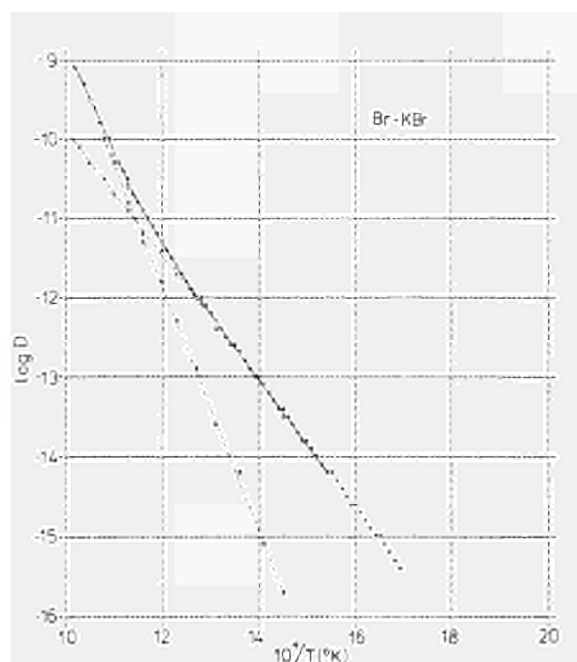


Fig. 18
Computer output of an iterative fit. The Arrhenius diagram contains the experimental points marked with "D", and the calculated low and high temperature processes as "A" and "B", respectively. The calculated fit is shown in asterisks.

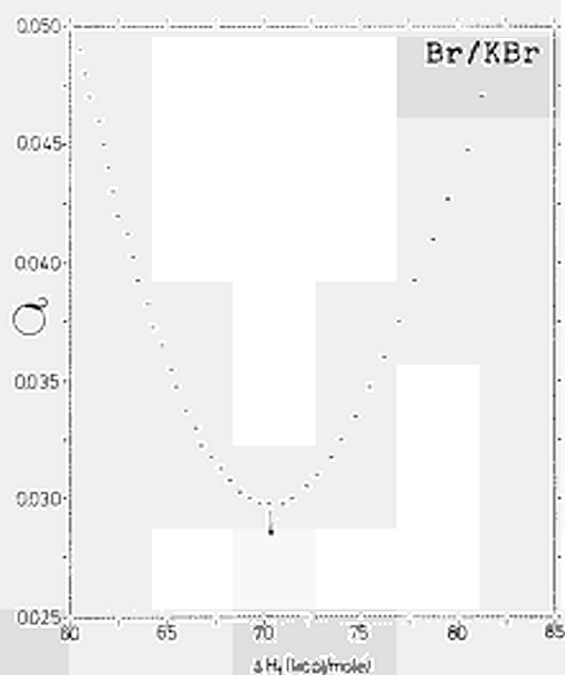


Fig. 19 : Plot of ΔH_1 versus σ for a "one-dimensional scan" for the data of Dawson and Barr on Br-diffusion in KBr.

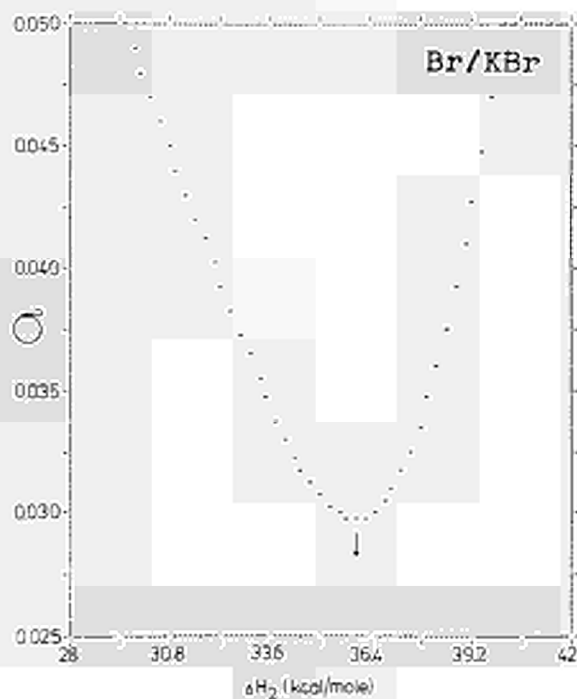


Fig. 20 : As above, but for ΔH_2 .

3. Diffusion of V and Ti in Ti by Murdock, Lundy, and Stansbury

These data were selected as typical for the anomalous behaviour of bcc metals, and because results were obtained over an extended temperature range thus yielding a clear definition of the low and the high temperature processes (see Figs. 21, 22 and Section 5.1.4 for possible interpretations). Due to the ratio of $\Delta H_1/\Delta H_2$ being less than that in the above two cases, the minima in one-dimensional fits (see Figs. 23-26) are less well defined, especially for ΔH_1 . A consistent best fit could nevertheless be obtained, which was in particular due to the high accuracy of the data, the extended temperature range, and the number of data points reported. If one or more of these features are lacking, a consistent fit is very difficult to be achieved or may not be achievable at all.

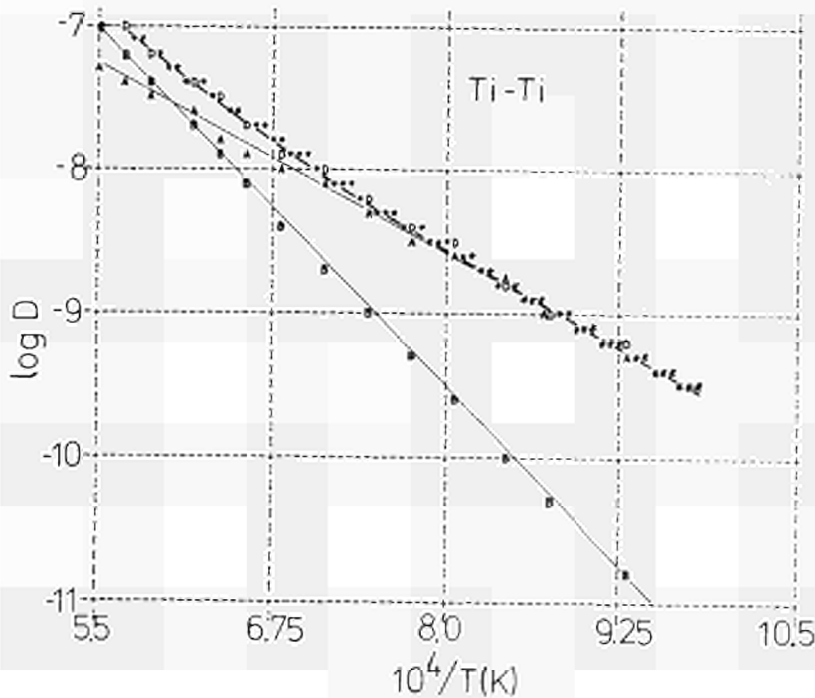


Fig. 21
Computer output of an iterative fit. The Arrhenius diagram contains the experimental points marked with "D", and the calculated low and high temperature processes as "A" and "B", respectively. The calculated fit is shown in asterisks.

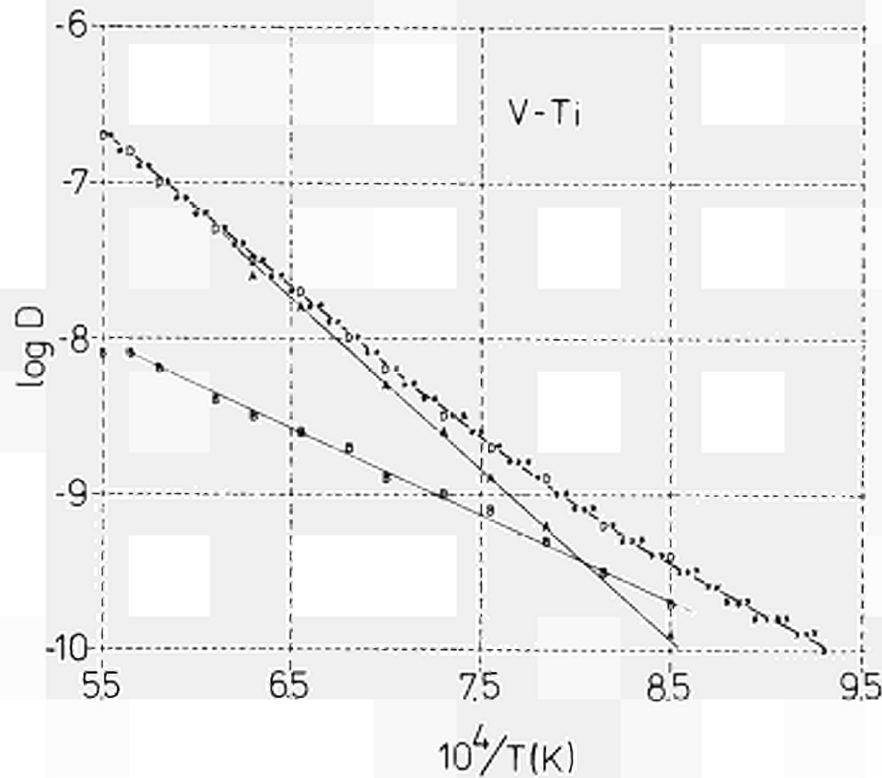


Fig. 22 : Computer output of an iterative fit. The Arrhenius diagram contains the experimental points marked with "D", and the calculated low and high temperature processes as "A" and "B", respectively. The calculated fit is shown in asterisks.

Further calculated fits are given in Tables VII and VIII. The best fits were obtained with the following sets of data

	ΔH_1 ΔH_2 (kcal/mole)	log $D_{0,1}$	log $D_{0,2}$	T_{inters} (°C)
present values	56.2 29.8	- 0.4	- 3.7	1446
authors' values	60.0 31.2	0.0	- 3.4	1550
present values	50.0 24.4	-0.7	- 5.1	1005
authors' values	57.2 32.2	0.1	- 3.5	1230

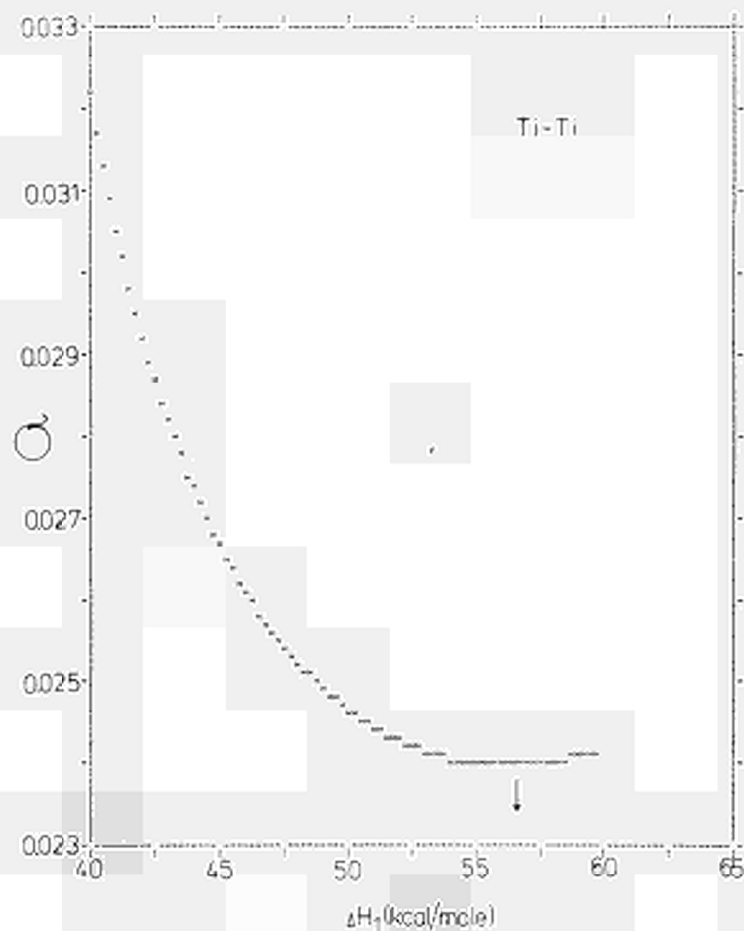


Fig. 23
Plot of ΔH_1 versus σ
for a "one-dimensional
scan" for Ti diffusion
in Ti. The symbols X
stand for iterative
fits.

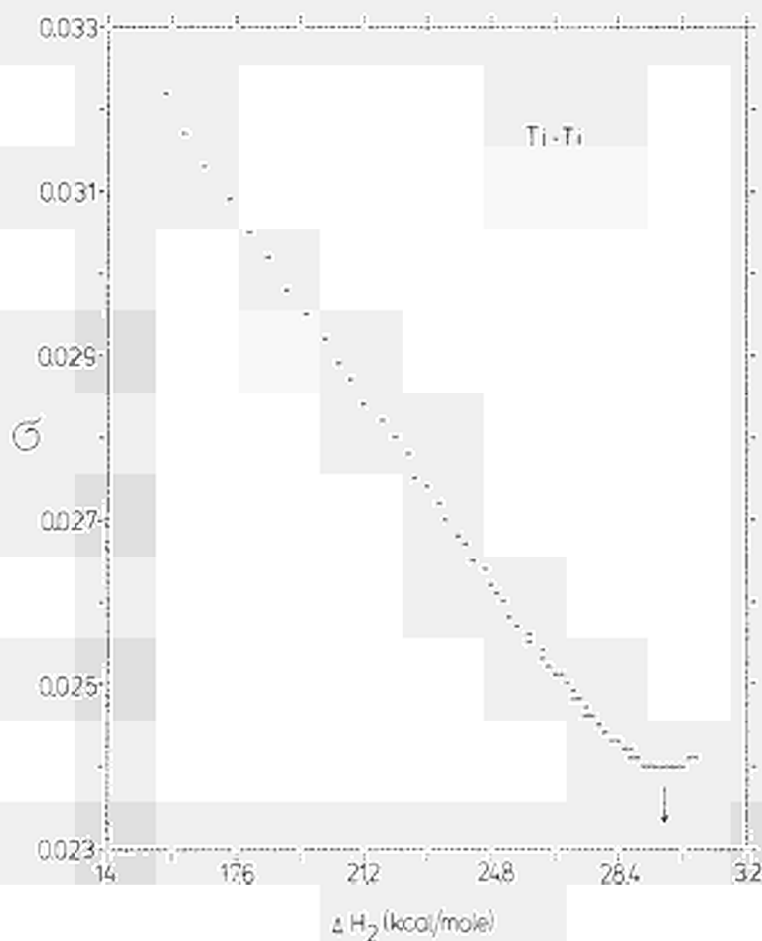


Fig. 24
As above, but for ΔH_2 .

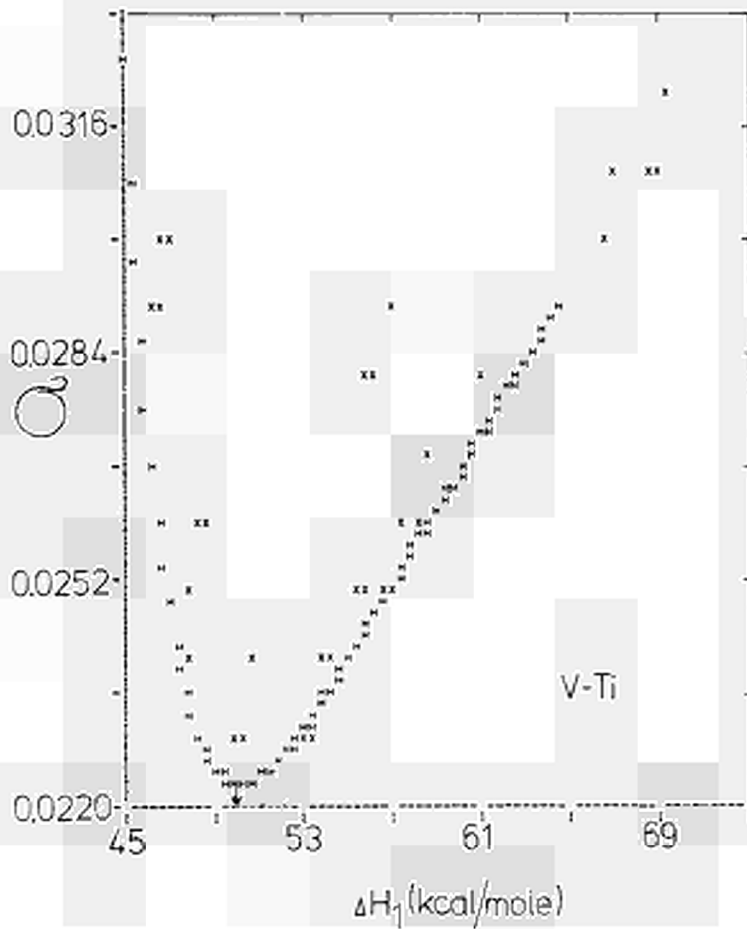


Fig. 25
Plot of ΔH_1 versus σ
for a "one-dimensional
scan" for V diffusion in
Ti. The symbols X stand
for iterative fits.

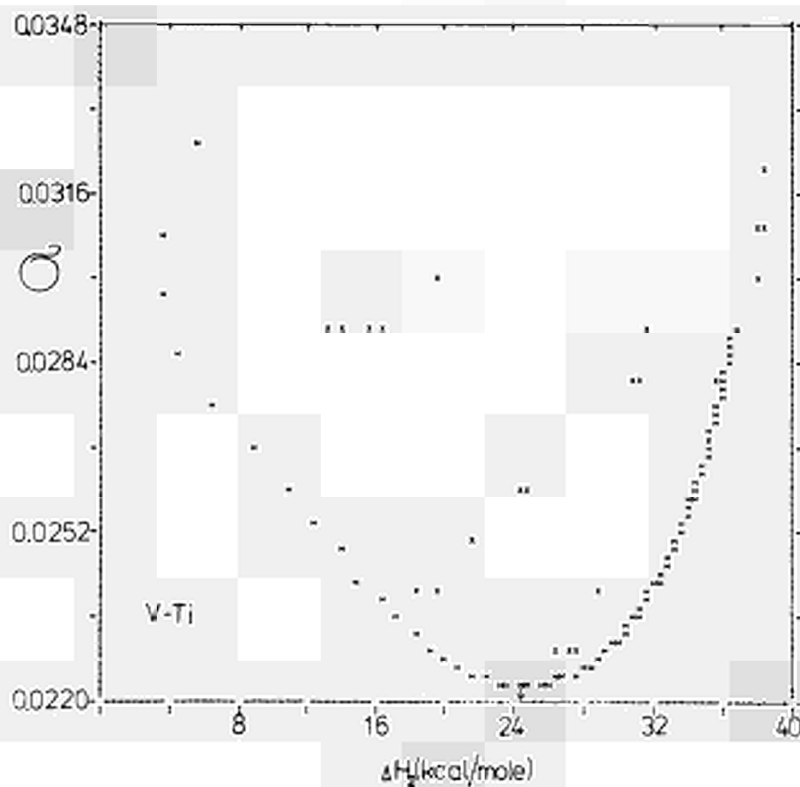


Fig. 26
As above, but for ΔH_2 .

Table VII

Calculated fits for the data of Murdock, Lundy, and Stansbury on Ti diffusion in Ti, ordered according to increasing standard deviation.

σ	ΔH_1	ΔH_2	$\log D_{0,1}$	$\log D_{0,2}$	T_{inters}
0.023973	56.25	29.75	-0.35	-3.72	1446
0.023974	56.00	29.67	-0.37	-3.73	1441
0.023974	56.50	29.81	-0.32	-3.71	1450
0.023976	55.75	29.61	-0.40	-3.74	1437
0.023977	56.75	29.87	-0.29	-3.69	1454
0.023980	55.50	29.55	-0.43	-3.75	1433
0.023981	57.00	29.93	-0.26	-3.68	1458
0.023986	55.25	29.47	-0.46	-3.77	1428
0.023987	57.25	29.99	-0.24	-3.67	1461
0.023994	55.00	29.41	-0.49	-3.78	1424
0.023995	57.50	30.04	-0.21	-3.66	1465
0.024004	54.75	29.34	-0.51	-3.80	1419
0.024004	57.75	30.10	-0.18	-3.65	1469
0.024015	58.00	30.15	-0.15	-3.64	1472
0.024016	54.50	29.27	-0.54	-3.81	1414
0.024027	58.25	30.21	-0.13	-3.63	1475
0.024030	54.25	29.20	-0.57	-3.82	1409
0.024041	58.50	30.26	-0.10	-3.62	1479
0.024046	54.00	29.12	-0.60	-3.84	1404
0.024056	58.75	30.31	-0.07	-3.61	1482
0.024065	53.75	29.03	-0.62	-3.86	1398
0.024072	59.00	30.36	-0.04	-3.60	1485
0.024085	53.50	28.96	-0.65	-3.87	1393
0.024090	59.25	30.41	-0.01	-3.59	1488
0.024108	53.25	28.88	-0.68	-3.88	1388
0.024109	59.50	30.46	0.01	-3.58	1491
0.024129	53.75	29.50	-0.04	-3.58	1494
0.024133	53.00	28.79	-0.70	-3.90	1382
0.024160	52.75	28.71	-0.73	-3.92	1377
0.024190	52.50	28.62	-0.76	-3.93	1371
0.024222	52.25	28.52	-0.79	-3.95	1364
0.024257	52.00	28.41	-0.81	-3.98	1357
0.024294	51.75	28.33	-0.84	-3.99	1352
0.024334	51.50	28.24	-0.87	-4.01	1346
0.024377	51.25	28.11	-0.89	-4.03	1338
0.024422	51.00	28.03	-0.92	-4.05	1332
0.024471	50.75	27.91	-0.95	-4.07	1325
0.024523	50.50	27.78	-0.98	-4.10	1317
0.024577	50.25	27.70	-1.00	-4.12	1311
0.024635	50.00	27.58	-1.03	-4.14	1304
0.024696	49.75	27.44	-1.06	-4.17	1296
0.024760	49.50	27.33	-1.08	-4.19	1288
0.024828	49.25	27.18	-1.11	-4.22	1280
0.024900	49.00	27.06	-1.14	-4.24	1272
0.024975	48.75	26.92	-1.17	-4.27	1264
0.025054	48.50	26.78	-1.19	-4.30	1256
0.025137	48.25	26.61	-1.22	-4.33	1247
0.025224	48.00	26.46	-1.25	-4.36	1238
0.025315	47.75	26.31	-1.27	-4.39	1230
0.025411	47.50	26.16	-1.30	-4.42	1221
0.025512	47.25	25.96	-1.33	-4.46	1211
0.025617	47.00	25.80	-1.35	-4.49	1203
0.025728	46.75	25.59	-1.38	-4.54	1193
0.025843	46.50	25.43	-1.41	-4.57	1184
0.025964	46.25	25.23	-1.44	-4.61	1175
0.026091	46.00	25.02	-1.46	-4.65	1165
0.026224	45.75	24.80	-1.49	-4.70	1155
0.026363	45.50	24.58	-1.52	-4.74	1145
0.026509	45.25	24.33	-1.54	-4.79	1135
0.026662	45.00	24.11	-1.57	-4.84	1125

Table VIII

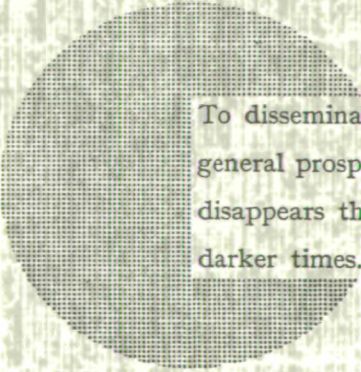
Calculated fits for the data of Murdock, Lundy, and Stansbury on V diffusion in Ti, ordered according to increasing standard deviation.

σ	ΔH_1	ΔH_2	$\log D_{o,1}$	$\log D_{o,2}$	T_{inters}
0.0223305	50.00	24.37	-0.67	-5.05	1005
0.0223306	50.25	24.99	-0.64	-4.93	1014
0.0223323	49.75	23.78	-0.70	-5.17	997
0.0223325	50.50	25.54	-0.61	-4.82	1023
0.0223358	50.75	26.05	-0.58	-4.72	1032
0.0223362	49.50	23.16	-0.73	-5.29	989
0.022404	51.00	26.54	-0.56	-4.63	1041
0.022426	49.25	22.47	-0.76	-5.43	981
0.022462	51.25	26.99	-0.53	-4.54	1050
0.022518	49.00	21.74	-0.79	-5.57	973
0.022529	51.50	27.42	-0.50	-4.45	1059
0.022606	51.75	27.85	-0.47	-4.37	1068
0.022642	48.75	20.95	-0.82	-5.72	965
0.022690	52.00	28.24	-0.44	-4.29	1077
0.022781	52.25	28.62	-0.42	-4.22	1087
0.022802	48.50	20.13	-0.85	-5.89	958
0.022878	52.50	28.98	-0.39	-4.15	1096
0.022980	52.75	29.32	-0.36	-4.08	1105
0.023003	48.25	19.20	-0.88	-6.07	950
0.023086	53.00	29.64	-0.33	-4.01	1114
0.023197	53.25	29.95	-0.31	-3.95	1123
0.023248	48.00	18.31	-0.91	-6.24	943
0.023311	53.50	30.25	-0.28	-3.89	1133
0.023428	53.75	30.54	-0.25	-3.84	1142
0.023548	54.00	30.81	-0.23	-3.79	1151
0.023550	47.75	17.04	-0.94	-6.49	936
0.023670	54.25	31.07	-0.20	-3.73	1160
0.023794	54.50	31.32	-0.17	-3.68	1169
0.023899	47.50	16.21	-0.97	-6.65	930
0.023919	54.75	31.56	-0.14	-3.64	1178
0.024047	55.00	31.79	-0.12	-3.59	1186
0.024175	55.25	32.02	-0.09	-3.55	1195
0.024304	55.50	32.23	-0.06	-3.51	1204
0.024318	47.25	14.89	-1.00	-6.91	924
0.024435	55.75	32.44	-0.04	-3.47	1212
0.024566	56.00	32.63	-0.01	-3.43	1221
0.024698	56.25	32.82	0.02	-3.39	1229
0.024803	47.00	13.82	-1.03	-7.12	918
0.024830	56.50	33.01	0.04	-3.36	1237
0.024962	56.75	33.19	0.07	-3.32	1245
0.025095	57.00	33.36	0.10	-3.29	1253
0.025228	57.25	33.52	0.12	-3.26	1261
0.025361	57.50	33.68	0.15	-3.23	1268
0.025536	46.75	12.29	-1.06	-7.41	912
0.025494	57.75	33.84	0.18	-3.20	1276
0.025527	58.00	33.98	0.21	-3.17	1283
0.025760	58.25	34.13	0.23	-3.14	1291
0.025893	58.50	34.27	0.25	-3.11	1298
0.026022	46.50	10.68	-1.09	-7.73	907
0.026025	58.75	34.40	0.29	-3.09	1305
0.026158	59.00	34.54	0.31	-3.06	1312
0.026290	59.25	34.66	0.34	-3.04	1318
0.026421	59.50	34.79	0.37	-3.01	1325
0.026553	59.75	34.91	0.39	-2.99	1332
0.026684	60.00	35.02	0.42	-2.97	1338
0.026784	46.25	8.64	-1.13	-8.12	902
0.026815	60.25	35.14	0.45	-2.95	1344
0.026945	60.50	35.24	0.48	-2.92	1350
0.027075	60.75	35.35	0.50	-2.90	1356
0.027204	61.00	35.45	0.53	-2.88	1362
0.027333	61.25	35.56	0.56	-2.87	1368
0.027461	61.50	35.65	0.58	-2.85	1373
0.027589	61.75	35.75	0.61	-2.83	1379

NOTICE TO THE READER

All scientific and technical reports published by the Commission of the European Communities are announced in the monthly periodical “**euro-abstracts**”. For subscription (1 year: B.Fr. 1 025,—) or free specimen copies please write to:

**Office for Official Publications
of the European Communities
Case postale 1003
Luxembourg 1
(Grand-Duchy of Luxembourg)**



To disseminate knowledge is to disseminate prosperity — I mean general prosperity and not individual riches — and with prosperity disappears the greater part of the evil which is our heritage from darker times.

Alfred Nobel

SALES OFFICES

The Office for Official Publications sells all documents published by the Commission of the European Communities at the addresses listed below, at the price given on cover. When ordering, specify clearly the exact reference and the title of the document.

UNITED KINGDOM

H.M. Stationery Office
P.O. Box 569
London S.E. 1 — Tel. 01-928 69 77, ext. 365

BELGIUM

Moniteur belge — Belgisch Staatsblad
Rue de Louvain 40-42 — Leuvenseweg 40-42
1000 Bruxelles — 1000 Brussel — Tel. 12 00 26
CCP 50-80 — Postgiro 50-80

Agency:
Librairie européenne — Europese Boekhandel
Rue de la Loi 244 — Wetstraat 244
1040 Bruxelles — 1040 Brussel

DENMARK

J.H. Schultz — Boghandel
Møntergade 19
DK 1116 København K — Tel. 14 11 95

FRANCE

*Service de vente en France des publications
des Communautés européennes — Journal officiel*
26, rue Desaix — 75 732 Paris - Cédex 15^e
Tel. (1) 306 51 00 — CCP Paris 23-96

GERMANY (FR)

Verlag Bundesanzeiger
5 Köln 1 — Postfach 108 006
Tel. (0221) 21 03 48
Telex: Anzeiger Bonn 08 882 595
Postscheckkonto 834 00 Köln

GRAND DUCHY OF LUXEMBOURG

*Office for Official Publications
of the European Communities*
Case postale 1003 — Luxembourg
Tel. 4 79 41 — CCP 191-90
Compte courant bancaire: BIL 8-109/6003/200

IRELAND

Stationery Office — The Controller
Beggars Bush
Dublin 4 — Tel. 6 54 01

ITALY

Libreria dello Stato
Piazza G. Verdi 10
00198 Roma — Tel. (6) 85 08
CCP 1/2640

NETHERLANDS

Staatsdrukkerij- en uitgeverijbedrijf
Christoffel Plantijnstraat
's-Gravenhage — Tel. (070) 81 45 11
Postgiro 42 53 00

UNITED STATES OF AMERICA

European Community Information Service
2100 M Street, N.W.
Suite 707
Washington, D.C., 20 037 — Tel. 296 51 31

SWITZERLAND

Librairie Payot
6, rue Grenus
1211 Genève — Tel. 31 89 50
CCP 12-236 Genève

SWEDEN

Librairie C.E. Fritze
2, Fredsgatan
Stockholm 16
Post Giro 193, Bank Giro 73/4015

SPAIN

Libreria Mundi-Prensa
Castello 37
Madrid 1 — Tel. 275 51 31

OTHER COUNTRIES

*Office for Official Publications
of the European Communities*
Case postale 1003 — Luxembourg
Tel. 4 79 41 — CCP 191-90
Compte courant bancaire: BIL 8-109/6003/200

CDNA05078ENC